GEOMICROBIOLOGY JOURNAL
https://doi.org/10.1080/01490451.2020.1812773

Taylor & Francis
Taylor & Francis Group

Tracing the Early Emergence of Microbial Sulfur Metabolisms

Patrick R. Morrison[a,b] and Stephen J. Mojzsis[b,c]

[a]Department of Ecology and Evolutionary Biology, University of Colorado, Boulder, CO, USA; [b]Department of Geological Sciences, University of Colorado, Boulder, CO, USA; [c]Research Centre for Astronomy and Earth Sciences, Institute for Geological and Geochemical Research, Hungarian Academy of Sciences, Budapest, Hungary

ABSTRACT

Hydrogen sulfide (nH_2S) and sulfur oxide (SO_n; $n = 1, 2, 3$) gases in early Earth's globally anoxic atmosphere were subjected to gas-phase chemical transformations by UV light. A principal photolysis pathway at that time produced elemental sulfur aerosols with mass-independently fractionated (MIF) isotopic values carrying variable minor isotope (^{33}S, ^{36}S) compositions. These rained into the sulfate-deficient Archean (ca. 3.85–2.5 Ga) oceans to react with $[Fe^{2+}]_{aq}$ and form sedimentary sulfides. The MIF-bearing sulfides were incorporated into Archean sediments, including banded iron formations (BIF). Such aerosols may also have fueled microbial sulfur metabolisms, and thus are traceable by the MIF sulfur isotopes. Yet, data show that before ~3.5 Ga mass-dependent $^{34}S/^{32}S$ values in Early Archean sediments tend to fall within a narrow (±0.1%) range even as they carry *mass-independent* values. By about 3.5 Ga, $^{34}S/^{32}S$ values show much greater changes (>1%) in range congruent with microbial metabolic processing. Here, we trace probable pathways of elemental sulfur aerosols into Archean sediments, and couple our study with analysis of the evolutionary relationships of enzymes involved in sulfur metabolism to explain the observed trends. Our model explains why elemental sulfur aerosols were apparently not utilized by the Eoarchean (pre-3.65 Ga) biosphere even though an immediate precursor to the required enzyme may have already been present.

HIGHLIGHTS

- Evolution of microbial sulfur metabolisms is tracked by multiple sulfur isotopes
- Alkaline hydrothermal vents were an abode for early microbial life
- Sulfite detoxification prompted anaerobic respiration
- Reversal of respiratory electron transport chain (ETC) stimulated photothiotrophy
- Surplus e- acceptors permitted the emergence of elemental sulfur reduction

ARTICLE HISTORY
Received 25 May 2020
Accepted 17 August 2020

KEYWORDS
Archean; mass-independent fractionation; microbial evolution; Sulfur isotopes

Introduction

Earth's biosphere is ancient, and its origin evidently predates the geologic record (Benner et al. 2020). Although the various lines of evidence for life's antiquity are debated, the fixation of organic carbon by biological activity from the earliest times is tentatively attested by the presence of ^{13}C-depleted carbonaceous matter captured within rocks of marine sedimentary origin dated to be about 3.8 Ga; low $^{13}C/^{12}C$ carbonaceous matter is a characteristic isotopic feature of metabolic activity associated with carbon fixation (Mojzsis et al. 1996; Rosing 1999; Schidlowski 1988; cf. Whitehouse et al. 2009). Other evidence, also strongly contested, for relatively sophisticated microbial communities before ca. 3.7 Ga include purported 'stromatolite-like' macrofossil shapes from ca. 3.71 Ga rocks in the Isua supracrustal belt of West Greenland (Nutman et al. 2016; cf. Allwood et al. 2018; Zawaski et al. 2020), and alleged 'microfossils' found within hydrothermal jaspilites of the ca. 3.78 Ga Nuvvuagittuq locality in Canada (Dodd et al. 2017; cf. Greer et al. 2020). Yet older and similarly strongly disputed hints of life are offered by ^{12}C-enriched graphite within rocks from the Nulliak assemblage in Labrador, Canada and assumed to be as old as ca. 3.95 Ga (Tashiro et al. 2017; cf. Whitehouse et al. 2019). Lastly, a few ca. 4.1 Ga zircons host inclusions of ^{12}C-enriched amorphous carbon (as hexagonal psuedomorphs after graphite) which offers the tantalizing prospect of an emergent Hadean biome (Bell et al. 2015; cf. Alleon and Summons 2019). Beyond these uncertain fossil traces from a patchy geological record, however, we have little direct knowledge of the operative metabolic style(s) that were present in the biosphere's first billion years. As it stands, there appears to have been a biosphere present on Earth by about 4 billion years ago that had the ability to fix organic carbon from inorganic sources. What was the nature of this microbial biosphere, and how could it have manifested itself in other ways?

CONTACT Stephen J. Mojzsis mojzsis@colorado.edu Department of Geological Sciences, University of Colorado, Boulder, CO, USA
Supplemental data for this article is available online at https://doi.org/10.1080/01490451.2020.1812773.

Antiquity of acetyl-CoA and its relationship to alkaline hydrothermal vents

One of the metabolisms most frequently argued to have present very early in the history of life is the reductive acetyl-coenzyme A (Acetyl-CoA), or Wood–Ljungdahl (W–L) pathway (e.g. Braakman and Smith 2012; Ragsdale and Pearce 2008). Biosynthesis via the autotrophic acetyl-CoA pathway uses free hydrogen from the environment as an electron donor, and carbon dioxide as an electron acceptor. The last universal common ancestors of all extant life (dubbed LUCA) are thought to have comprised a population which used this W–L pathway in a primordial H_2-powered biosphere, perhaps associated with hydrogenous alkaline hydrothermal settings (e.g. Weiss et al. 2016). We return to this setting later in our analysis. Meanwhile, it is important to note that the LUCA organism(s) had already reached a level of complexity which places them far from the origin of life, perhaps in the late Hadean. Further, going beyond the debate over whether or not life actually originated in hydrothermal vents on the seafloor or, alternatively in shallow settings on dry land, evidence from molecular phylogenies points to hydrothermal vents as at least a waystation in early life's history from its origins to the crystallization of the genome that preceded Bacteria, Archaea, and Eukarya (Pace 2006).

Still, a strong argument for at least a *syn-* or perhaps even *pre*-biotic origin of the acetyl-CoA pathway comes from experiments that show native transition metals (Fe^0, Ni^0, Co^0) can, under natural conditions, selectively reduce CO_2 to $CH_3CO_2^-$ and $C_3H_4O_3$ (acetate and pyruvate, respectively; Varma et al. 2018). More recently, Preiner et al. (2020) showed that acetate and pyruvate are also formed under alkaline hydrothermal conditions from H_2 and CO_2—as in the biological pathway—using only mixed-valence Fe(±Ni) oxides in water as the catalyst. Analysis also suggests that these ancient intermediates and end-product compounds of W–L pre-date LUCA (e.g. Goldford et al. 2019).

Native metals and alloys (e.g. $Ni_{2,3}Fe$; awaruite) are well known as mineralogical products of serpentinized peridotite within hydrothermal systems (Sousa et al. 2018). Furthermore, certain minerals of the Osmiridium-group (Os-Ir-Ru-Pt alloys) occur in serpentinized ultramafic rocks and their weathering detritus (e.g. Hattori and Cabri 1992). Briefly, serpentinization is the hydration of (peridotitic) olivine $(Mg,Fe)_2SiO_4$, and orthopyroxene (Mg, Fe, Ca) (Mg, Fe, Al) (Si, Al)$_2O_6$. A general form of the serpentinization reaction involves the hydration reaction of olivine to form serpentine, magnetite and free hydrogen:

$$6[(Mg_{1.5}Fe_{0.5})SiO_4] + 7H_2O \rightarrow 3[(Mg_3Si_2O_5(OH)_4)] + Fe_3O_4 + H_2 \quad (1)$$

Significantly, these reactions exist wherever hot ultramafic rocks are in contact with water; they provide a reducing environment with high H_2 concentrations where native metals catalyze hydrocarbon production with H_2 as the electron donor (e.g. Proskurowski et al. 2008). We view this as a compelling natural chemical reactor space that provides a prebiotic route to the origin of the W–L pathway and comports with the logical arguments provided in Russell and Martin (2004).

Aside from serving as a cradle for the early biosphere, widespread hydrothermal emanations from the extensive hot Archean seafloor crust dictated to no small degree the composition of early Earth's seawater. For example, rare earth element studies show that the plentiful Fe^{2+} present in the Archean (3.85–2.5 Ga) originated primarily from the expulsion of metalliferous hydrothermal vent fluids (Jacobsen and Pimentel-Klose 1988).

Taken together, it is unmistakable that the widespread hydrothermal environments on the primordial Earth provided a ready supply of native metals, simple organic molecules, and free hydrogen to power one of the stepping stones in the history of early life from its origin (someplace) to ultimate colonization of the global ocean. We posit that—at the least—an intermediate stage of life must have included residence around hydrothermal vents, that the vents were the primary sources of reactive iron (II) to account for the deposition of the ubiquitous banded iron formations (e.g. Posth et al. 2013; Mineralogical aspects of microbial 'sulfate reduction' section), and that the combined geochemistry of the sulfur isotopes in the oldest known sediments and phlyo-metabolic data is a testimony to this history.

Apart from carbon isotope studies of the oldest rock of sedimentary origins cited above, fractionations in the relative isotopic abundances of the other principal biophilic elements (Fe, N, and S; e.g. Thomazo et al. 2009 and references therein) are widely used to imply that a globally active biosphere was present in the first billion years. Among these, the stable isotopes of sulfur (^{32}S, ^{33}S, ^{34}S, ^{36}S) stand out as a versatile tool for the elucidation of oxidation modes and the metabolic styles of microbial communities in deep time (e.g. Johnston 2011).

Sulfur isotope geochemistry as a tracer of ancient environments and metabolisms

The many geomicrobiological insights provided by sulfur ultimately emanate from variations in its 8 (−II to + VI) valence states (Figure 1). This is reflected in a rich metal-sulfur chemistry and mineralogy, as well as the isotopic composition in sulfur-containing minerals found in sedimentary rocks. These variations reflect the different partitioning of its four stable isotopes into various compounds via certain biochemical reactions under different environmental regimes. Technically, such induced variation is termed 'stable isotope fractionation'. Specific biochemical reactions associated with different microbial metabolic styles can thus produce compounds with characteristic sulfur isotopic ratios that are interpretable if the source isotopic composition and reaction pathways are known (or inferred). In this way, it becomes possible to use the isotopic compositions of sedimentary sulfur minerals to pinpoint metabolic styles in the geologic record.

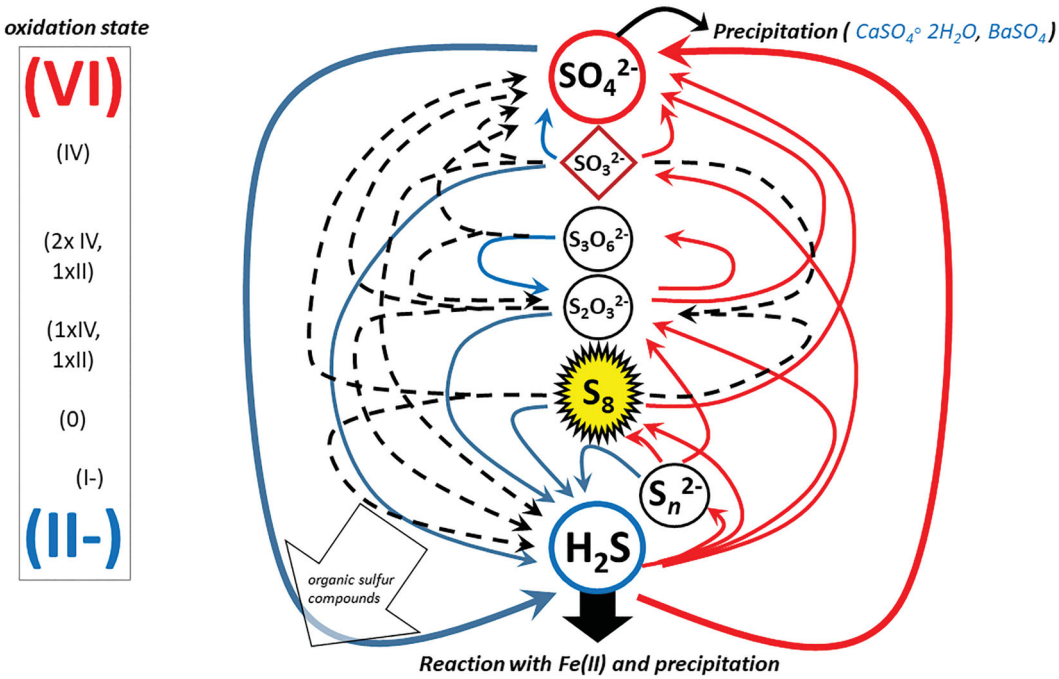

Figure 1. Schematic diagram of the sedimentary sulfur cycle with reductive (blue line at left, downward arrows) and oxidative (red line at right, upward arrows) pathways illustrated with respect to valence state (−II to + VI). Dashed lines in the reductive regime (LEFT) represent microbial disproportionation reactions. In this representation, the sulfur cycle is powered either by degradation of organic matter via sulfate-reducers (heavy blue arrow), or sulfide oxidation (heavy red arrow), or intermediate pathways such as elemental sulfur (aerosol; S_8 reduction/oxidation). Sedimentation and burial of ferrous-sulfide minerals (mostly FeS_2; but see Figure 3 which includes intermediate mackinawite and greigite) is the dominant sink for reduced sulfur in the marine sedimentary system (modified after Zopfi et al. 2004). (For interpretation of the references to color in this figure legend, the reader is referred to the web version of this article.).

The approach to using sulfur isotopes in this way has a long history (e.g. Monster et al. 1979; Schidlowski et al. 1983; Strauss 1993, 1997, 2003). As reviewed elsewhere (e.g. Mojzsis 2007) surface geochemical cycling of sulfur from the beginning of the continuous geologic record at ca. 3.85 Ga (Nutman et al. 1997) to the rise of atmospheric oxygen around 2.42 Ga (Papineau et al. 2007) is understood to have been dominated by atmospheric reactions under neutral and anoxic conditions (Farquhar et al. 2000, 2001; Pavlov and Kasting 2002). These UV-generated gas phase reactions ('Atmospheric photochemistry and multiple sulfur isotopes' section) produced sulfur compounds with anomalous enrichments and depletions in the minor sulfur isotopes (^{33}S, ^{36}S) and can be preserved in the rock record (e.g. Farquhar and Wing 2003). Long-term variations in these sulfur isotope signatures and the timing of their appearance (and *disappearance*) from the geologic record are now routinely used to analyze atmospheric chemical changes over geologic timescales and, important for this work, the early evolution of the surface zone up to the Paleoproterozoic era (2.5–1.6 Ma; e.g. Kumar and Francisco 2016). In particular, the last two decades have focused on using this powerful multifarious sulfur isotopic tool (MDF/MIF) to determine the timing of the irreversible oxygenation of the surface zone at the Great Oxidation Event at ca. 2.42 Ga (Holland 2006; Kaufman et al. 2007; Papineau et al. 2007).

A less-exploited component of the Earth's early sulfur cycle is to study how observed changes in both the magnitude of anomalous minor isotope (^{33}S) enrichments and depletions, along with changes in the absolute ranges of $^{34}S/^{32}S$, relate to metabolic innovations that appeared at different times owing to changes in local as well as global selection pressures. The review by Thiemens and Lin (2019) provides the appropriate background information of this chemistry to begin to make sense of how we can trace the emergence of life with this interesting chemistry.

Here, we direct our attention to the multiple sulfur isotope geochemistry for which data exist for the world's oldest sediments—mostly comprised of the BIFs—followed by an overview of the isotopic fractionation processes believed to be involved in the Archean biosphere. We explain how the sulfur isotopic signatures produced by these processes can be used as tracers of the pathways of elemental sulfur to the microbial biosphere and to follow its subsequent modifications. To explain the observed mass-dependent and mass-independent multiple sulfur isotopic trends in the earliest geologic records of marine sedimentary sulfides, we suggest that is was not until about 3.5 Ga that microbes began to widely make use of elemental sulfur as an electron acceptor in metabolism. Prior to that time, our interpretation of the isotopic evidence posits that such a metabolism had not yet evolved even if an immediate precursor already existed. We further propose that the advent of anoxygenic photosynthesis provided an excess of electron acceptors in the form of organic carbon sometime between 3.7 and 3.5 Ga which offered the necessary evolutionary changeover for microbes to use elemental sulfur aerosols in new ways. Our work concludes with recommendations that the 'missing' 200 Myr multiple sulfur isotope record between 3.7 and 3.5 Ga be unveiled to pinpoint when photothiotrophy (the photosynthesis pathway that utilizes sulfur as the e-donor) may have originated.

Reporting multiple sulfur isotope heterogeneities in the geologic record

We now review the theoretical considerations in reporting multiple sulfur isotope data. This section provides—in brief—the basis of isotopic geochemistry arguments (see Thiemens and Line 2019) for tracing the emergence of microbial sulfur metabolisms using data reported from the geologic record, and relate these changes to broader-scale transformations to the geosphere.

Conventional notations for the multiple sulfur isotopes

The four stable isotopes of sulfur (^{32}S, ^{33}S, ^{34}S, ^{36}S) have the approximate terrestrial abundances of 95.03, 0.7487, 4.197, and 0.01459%, respectively (Ding et al. 2001). These specific isotopic abundances were determined prior to the formation of our solar system via nucleosynthesis reactions in stars before they became incorporated into the building blocks of the planets (Mojzsis 2007). In reporting the chemistry of mass-dependent fractionation of multiple isotopes such as sulfur (e.g. Domagal-Goldman et al. 2011), we let a and b label the specific S isotopes, ^{a}S and ^{b}S, with a or b = [32, 33, 34, 36] as shown above, and $a \neq b$. In the hypothetical isotopic substitution reaction: $^{a}SA + {}^{b}SB \rightleftarrows {}^{b}SA + {}^{a}SB$ the equilibrium constant is expressed as:

$$K_{eq}^{ab} = \exp\left(-\frac{\Delta E_{ab}}{kT}\right) = \frac{[^{b}SA]_{eq}[^{a}SB]_{eq}}{[^{a}SA]_{eq}[^{b}SB]_{eq}}. \quad (2)$$

Here, $\Delta E_{ab} = E(^{b}SA) + E(^{a}SB) - E(^{a}SA) - E(^{b}SB)$ is the free energy difference between reactant and product. From zero-point-energy arguments, it can be shown that $\Delta E_{ab} \propto \left(1/\sqrt{m_a} + 1/\sqrt{m_b}\right)$. Since ^{32}S is the lightest and most abundant isotope, we take it as the reference, so that $a = 32$. When comparing three isotopes (e.g. ^{32}S, ^{33}S, ^{34}S) and because the mass differences of the isotopes are small, an approximation can be made:

$$\Delta E_{ab}/\Delta E_{ac} \approx (1/m_a - 1/m_b)/(1/m_a - 1/m_c) = \lambda_{eq}. \quad (3)$$

To report differences in the ratios of two isotopes (usually the most abundant, here ^{32}S and ^{34}S), the conventional delta (δ) notation is used for mass-dependent isotopic fractionations. The mass-dependent sulfur isotopic compositions are expressed as part-per-thousand (0.1%; 1/1000; per mille; ‰) variations relative to a reference standard, as follows:

$$\delta^{b}S = \left[\frac{(^{b}SA/^{32}SA)_{\text{sample}}}{(^{b}SA/^{32}SA)_{\text{standard}}} - 1\right] \times 1000 \quad (4)$$

Where (Equation 4) b may refer to 33, 34, or 36, and δ^{b}S is reported in units of ‰. The standard reference, which by definition is 0.00‰, is Vienna Cañon Diablo Troilite (VCDT). The VCDT standard is presently defined relative to a Ag-sulfide reference IAEA-S-1 with an agreed $\delta^{34}S_{VCDT}$ value of −0.3‰.

Mass-dependent fractionations (MDF) represent the majority of processes within the sulfur isotope system. In MDF the isotopic ratios—(^{34}S/^{32}S), (^{33}S/^{32}S), (^{36}S/^{32}S)—show systematic variability in proportion to the mass differences between the isotopes (Urey 1947; Hulston and Thode 1965). Hence, variations in (^{33}S/^{32}S) of a sulfur-containing sample will be slightly more than half of that of (^{34}S/^{32}S) for the same sample. This is because of the mass difference between ^{33}S and ^{34}S is the nucleon mass/energy difference between a neutron and a proton ($M_p = 0.99862349\,M_n$). The resulting linear fractionation trends, commonly termed the terrestrial mass fractionation lines (TMFL), emerge from this mass difference with a slope of slightly more than 0.5:

$$\delta^{33}S = 0.515 \times \delta^{34}S \quad (5.1)$$

$$\delta^{36}S = 1.91 \times \delta^{34}S \quad (5.2)$$

Before the work of Farquhar et al. (2001), almost all sulfur isotope studies measured only (^{34}S/^{32}S) because it was not expected that deviations in (^{34}S/^{32}S) vs/(^{33}S/^{32}S) would occur in the rock record (cf. Thode et al. 1949; Riciputi et al. 1998). It is now widely understood that isotopic compositions that deviate significantly from the TMFL are preserved even in the oldest BIFs (e.g. Mojzsis et al. 2003). The deviations reflect mass-independent fractionation (MIF) processes of the S isotopes, and the Capital Delta (Δ) values are used to document this phenomenon. The definition for this phenomenon requires a second reference isotope, taken to be ^{34}S. The general form is:

$$\Delta^{b}S = \delta^{b}S - [(1 + \delta^{34}S)^{{}^{b}\lambda_{eq}} - 1], \quad (6)$$

Where $^{b}\lambda_{eq} = (1/m_{32} - 1/m_b)/(1/m_{32} - 1/m_{34})$. We know, $^{b}\lambda_{eq} = \lambda_{eq}$ (Equation 3), and with the appropriate reference isotopes, $a = 32$ and $c = 34$; the mass differences lead to a slope value $^{33}\lambda_{eq} = 0.515$.

As with δ values, MIF is expressed in the conventional notation on terms of $\Delta^{33}S$ and $\Delta^{36}S$ in parts-per-thousand (‰) deviations from the standard $^{33}\lambda_{eq}$ slope, as:

$$\Delta^{33}S = \delta^{33}S - 1000 \times \left[\left(1 - \frac{\delta^{34}S}{1000}\right)^{0.515} - 1\right] \quad (7.1)$$

$$\Delta^{36}S = \delta^{36}S - 1000 \times \left[\left(1 - \frac{\delta^{34}S}{1000}\right)^{1.91} - 1\right] \quad (7.2)$$

Somewhat like the δ-notation, *positive* $\Delta^{b}S$ values ($+\Delta^{33}S$ and $+\Delta^{36}S$) indicate that a compound is anomalously enriched in that minor isotope, whereas a negative value points to depletion. The processes of MIF were so important on Earth prior to the GOE that it is misleading to term them as anomalous; these are reviewed below. Furthermore, although it seems that the sulfur MDF connotes $\Delta^{b}S_{eq} = 0$, we know that small differences in$\Delta^{b}\lambda_{eq}$ can exist with different MDF processes or different standards (including VCDT) and different types of fractionations both abiotic and biotic (e.g., Farquhar et al. 2003). The inorganic reference materials show a narrow range in $\Delta^{33}S$ of ±0.1‰ (2σ) about 0‰. For example, Papineau et al. (2005) explained that this natural scatter in the standards statistically exceeds the internal analytical precision of the measurements. They proposed that these reflect additional sources of error, or the scatter

may reflect real heterogeneity resulting from different modes of mass-dependent fractionation among the standards (Young et al. 2002). Values which fall more than 3σ beyond a band in the TMFL about $\pm 0.1‰$ from $\Delta^{33}S = 0‰$, are interpreted as a signal of MIF.

MDF and MIF fractionation processes documented in the Archean sulfur cycle

Different modes of isotopic fractionation produce sulfur compounds with diverse isotopic compositions, and that the combination of measured multiple isotopes (δ, Δ) described in 'Atmospheric photochemistry and multiple sulfur isotopes' section can be used to identify the activity of these processes in deep time. Here, we turn our attention to some fractionation processes understood to have existed in the Archean surface sulfur cycle, the different isotopic signatures produced by those processes and how they can be understood in relation to the evolution of microbial metabolisms that utilize sulfur (either in reduced or oxidized form). While other fractionation processes are thought to have been active in Archean time, our discussion concerns those which are most relevant to understanding the early evolution of elemental sulfur utilization by life.

Atmospheric photochemistry and multiple sulfur isotopes

Laboratory control experiments have shown that MIF sulfur isotopic signatures are produced by photolysis reactions with SO and SO_2 gas under ultraviolet lamps with wavelengths in the broadband 185–220 nm wavelengths under strictly anoxic atmospheres (Farquhar et al. 2000, 2001; Farquhar and Wing 2003). Modeling studies have sought to understand better the underlying mechanisms of this photochemistry in the Archean (Claire et al. 2014; Lyons 2009). These processes include photo-dissociation and/or photoexcitation (Lyons 2009). Authigenic sedimentary sulfur minerals (sulfides and sulfates) typically show characteristic non-zero $\Delta^{33}S$ and $\Delta^{36}S$ values, where $\Delta^{36}S/\Delta^{33}S \approx -0.90$, and $\Delta^{33}S/\delta^{34}S \approx +0.73 \pm 0.15$ (Farquhar et al. 2001; Farquhar and Wing 2003; Thomassot et al. 2015); these slopes are referred to as the Archean Reference Arrays (ARA; Figure 2). It should be noted, however, that although the ARAs are commonly viewed as reliable MIF sulfur signals, other studies continue to investigate non-atmospheric causes for this phenomenon including reaction in aqueous solution or organic + aqueous mixtures (e.g. Kumar and Francisco 2016; Lasaga et al. 2008; Watanabe et al. 2009; Whitehill and Ono 2012).

Other mechanisms of atmospheric MIF sulfur production—besides the broadband ~200 nm UV array—have been explored to explain the records found in ancient rocks (Lyons 2009). Beyond the ARA mentioned above, further experimental and numerical mechanisms for the various $\Delta^{33}S/\delta^{34}S$ slope trends labeled in Figure 2 that can be identified over the course of the Archean eon can be summarized as follows (Claire et al. 2014; Thomassot et al. 2015):

i. photo-dissociation with self-shielding in a SO_2-N_2 gas [$\Delta^{33}S/\delta^{34}S = +0.086 \pm 0.035$ (Ono et al. 2013)]
ii. photo-excitation [$\Delta^{33}S/\delta^{34}S \approx +0.5$ (Hattori et al. 2013)]
iii. photo-excitation of self-shielded SO_2 molecules in the 240 to 350 nm range [$\Delta^{33}S/\delta^{34}S$ from ~+1 (Whitehill and Ono 2012) to +3 (Ono et al. 2013)].

Corroborating evidence for a gas phase origin of these anomalous signatures also come from the observation of similar values in modern atmospheric sulfate aerosols and in sulfate from volcanogenic SO_n from Antarctic ice, in some cases these are correlated to historical volcanic eruptions that deliver sulfur gases to the stratosphere (Baroni et al. 2007; Romero and Thiemens 2003; Savarino et al. 2003). Owing to this body of evidence, photochemical transformations of SO_n are widely accepted as the cause of Archean MIF sulfur signatures even if other media are possible (cf. Kumar and Francisco 2016). The analyzed products—reduced and oxidized sulfur aerosols—of this UV induced photochemistry giving MIF S provide isotopic mass balance. The oxidized aerosol in this case, sulfate (SO_4^{2-}), partitions sulfur isotopes such that it carries *negative* $\Delta^{33}S$ and *positive* $\Delta^{36}S$ values. Contrariwise, elemental sulfur aerosols (S^0, S_{n+1}, cyclic S_8, polymeric S; Steudel 2003) carry *positive* $\Delta^{33}S$ and *negative* $\Delta^{36}S$. We refer the reader to Claire et al. (2014) and Thomassot et al. (2015) for more about these phenomena.

Archean MIF sulfur aerosols, atmosphere transparency, low pO_2, and scattering

As mentioned previously, controlled experiments show that low intrinsic oxygen concentrations and specific UV wavelengths that penetrated deep into the atmosphere are required to produce and preserve widespread MIF sulfur signatures in the geologic record. Ozone and oxygen are the primary absorbers of UV at wavelengths less than 300 nm, including those wavelengths involved in the photochemical reactions described in the previous section.

To account for the observed pervasive MIF sulfur in the pre-GOE geological record and its continuum from the end of the Hadean to the Paleoproterozoic (with the possible exception of the Mesoarchean; Thomassot et al. 2015), Mojzsis (2007) argued that Earth's atmosphere must have had the following properties: (i) transparent to short wavelength UV radiation and not so dense (e.g. $\ll 0.5$ bar CO_2) that Einstein-Smoluchowski scattering attenuates UV photons and prevent them from penetrating deep into the atmosphere; and (ii) low in atmospheric pO_2 to mitigate the formation of an ozone screen, as well as to prevent the production of significant marine sulfate to dilute a MIF sulfur signal. Pavlov and Kasting (2002) calculated that the effective transfer of MIF via reduced sulfur species (S^0 to polymeric S_{n+1}) from the atmosphere to the oceans requires that the early atmosphere had pO_2 values $\ll 10^{-5}$ present atmospheric levels (Lyons et al. 2014).

The undoubtedly abundant MIF S_{n+1} aerosols in the Archean serve as excellent tracers of the early evolution of the biogeochemical sulfur cycle, and we use this fact to explain $\Delta^{33}S/\delta^{34}S$ data in the context of the emergence of different styles of metabolic cycling of sulfur. We now direct

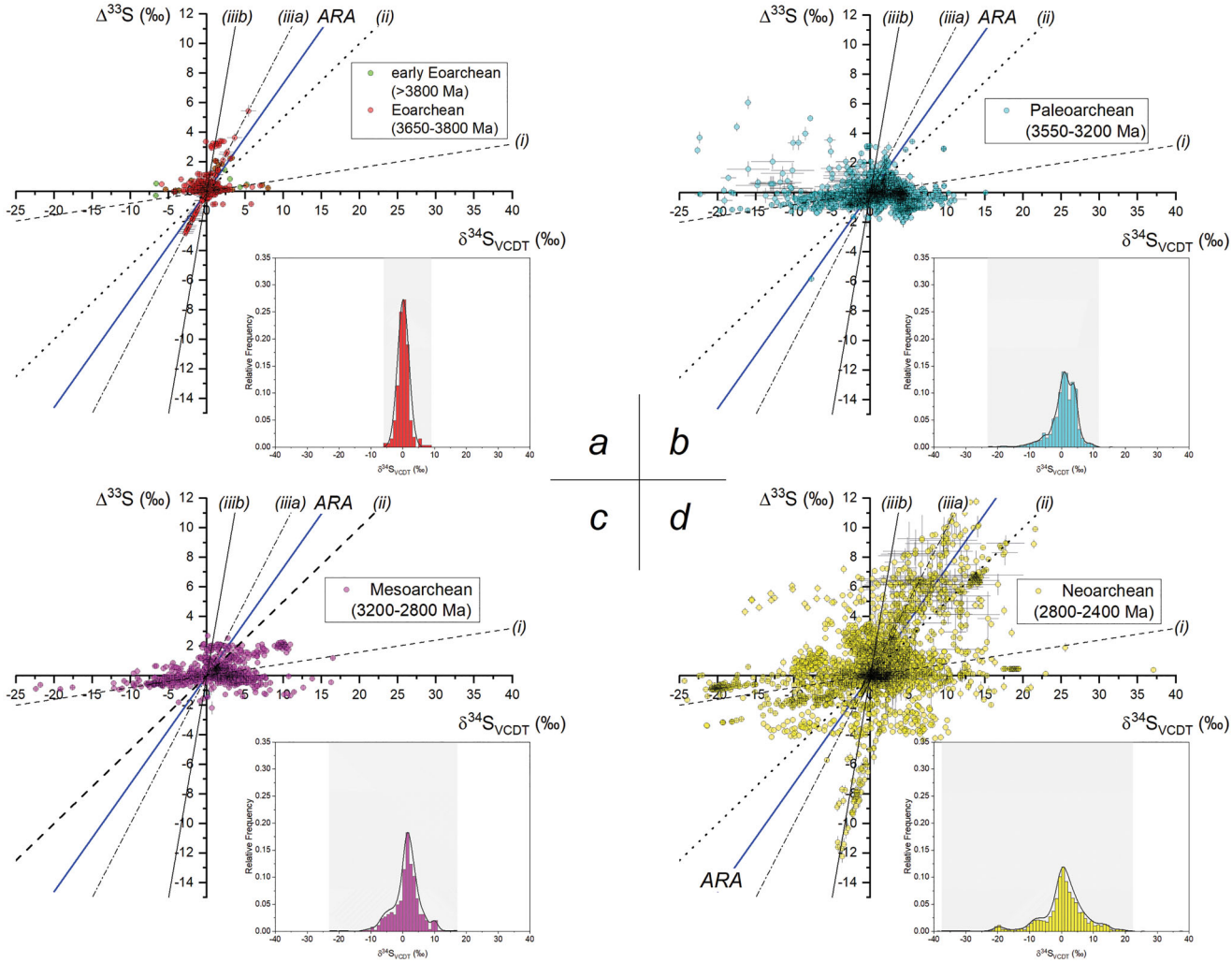

Figure 2. The multiple sulfur isotope record of the different stages of the Archean. Here, we assess the relative influence of the different mass-independent fractionation trends via the $\delta^{34}S$ vs. $\Delta^{33}S$ relationship. The data are binned by age (a–d); generally, most mass-dependent Eoarchean data plot with $\delta^{34}S$ near zero (inset, a), whereas ever increasing spreads in range of mass-dependent fractionation values as shown in the inset histograms characterize the Paleoarchean/Mesoarchean (similar) and Neoarchean records. a: $\delta^{34}S$ vs. $\Delta^{33}S$ data for Eoarchean [3650–3830 Ma], b: Paleoarchean [3200–3650 Ma], c: Mesoarchean [2800–3200 Ma], d: Neoarchean/early Paleoproterozoic [2400–2800 Ma]). Sulfur mass-dependent fractionation is expressed as $\delta^{34}S_{VDCT}$ on the x-axis, whereas mass-independent fractionation is reported in $\Delta^{33}S$ on the y-axis. Also shown are the various documented mechanisms of atmospheric MIF sulfur production (see text, 'Atmospheric photochemistry and multiple sulfur isotopes' section). Labeled here are: ARA = Archean reference array; (i) photo-dissociation with self-shielding in a SO_2–N_2 gas; (ii) photo-excitation; (iiia) photo-excitation of self-shielded SO_2 molecules in the 240–350 nm range from Whitehill and Ono (2012) and (iiib) from Ono et al. (2013). Data and sources are provided in Supplementary Online Materials. (For interpretation of the references to color in this figure legend, the reader is referred to the web version of this article.).

our attention in this work to elemental sulfur aerosols that carry *positive* $\Delta^{33}S$ and for which the most MIF S data are available; we therefore limit further discussion to the $\Delta^{33}S$/$\delta^{34}S$ system. At the present time, the $\Delta^{36}S$ systematics are still limited as long as relatively fewer data are available for $^{36}S/^{32}S$ for ancient rocks.

Archean sulfur metabolisms

Of the various microbial sulfur metabolisms proposed to have been active in the Archean eon (e.g. Eickmann et al. 2018; Guy et al. 2012; Shen et al. 2001, 2009; Wacey et al. 2010), we direct our analysis to the *sulfur reducers*, *oxidizers*, and *disproportionators* (*elemental sulfur fermenters*). We refer the reader to recent reviews (e.g. Maier 2014) for more details about the nature of the sulfur biogeochemical cycles, to Rabus et al. (2013) for sulfur metabolisms and to Dahl (2017) for a comprehensive analysis of phototrophic sulfur metabolism.

Mineralogical aspects of microbial 'sulfate reduction'

'Sulfate-reducing' microbes actually metabolize SO_4^{2-} transformed to SO_3^{2-} by ATP activation, or formation of sulfite (and bisulfite; HSO_3^-) by reaction of SO_2 in water, to produce product sulfide- and polysulfide (S_n^{2-}) that in turn reacts in water to form metal sulfide (Figure 3: Mineralogical aspects of microbial 'sulfate reduction' section). This subsequently goes on to become incorporated into sediments. The general exergonic part of sulfate reduction is sulfite reduction (or sulfur reduction) to H_2S. In the

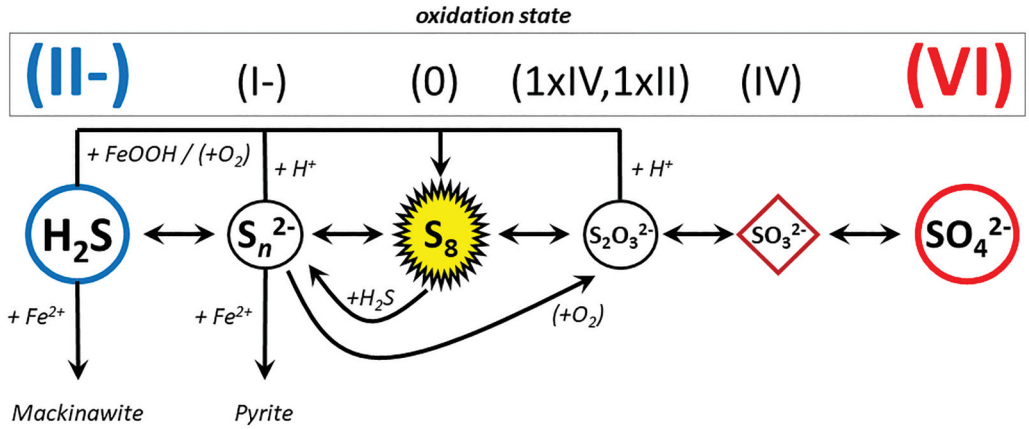

Figure 3. Schematic diagram of inorganic sulfur redox reactions in the marine system related to source and valence state (see Figure 1). The central role of elemental sulfur/polysulfide (aerosol) in controlling intermediate sulfur species transitions as well as Fe-sulfide mineralization is emphasized in this conceptual framework (modified from Kafantaris and Druschel 2020). (For interpretation of the references to color in this figure legend, the reader is referred to the web version of this article.).

geobiological literature, this reaction is commonly expressed as:

$$2CH_2O + SO_4^{2-} \rightarrow H_2S + 2HCO_3^- \quad (8)$$

where CH_2O is taken as generic 'organic matter' (Berner 1984) and the implication is that SO_2 forms SO_3^{2-} which can also be used in lieu of SO_4^{2-}. Microbes that perform microbial sulfate reduction (MSR) preferentially metabolize ^{32}S-compounds relative to ^{34}S-compounds, which leads to mass-dependent depletions in ^{34}S vs. ^{32}S and consequently negative fractionations in the $\delta^{34}S$ of the product sulfide (Harrison and Thode 1958; Jones and Starkey 1957; Thode et al. 1951). Analysis of modern sedimentary environments shows that these isotopic fractionations can be up to ~50‰ (Canfield 2001; Goldhaber and Kaplan 1975).

Sulfide minerals can be produced by the reaction of MSR-produced H_2S (Equation 8) with $Fe(II)_{aq}$ to form precursor amorphous $[FeS]_{aq}$ and thence to intermediates such as mackinawite ($(Fe,Ni)_{1+x}S$ (where $x = 0$–0.11)) which transforms at low temperature diagenesis to greigite ($(Fe^{2+}Fe^{3+})_2S_4$), and the orthorhombic polymorph marcasite (FeS_2) to the cubic mineral (FeS_2) pyrite (e.g. Schoonen and Barnes 1991; Avetisyan et al. 2019). Sulfur metabolically processed in MSR means that these minerals preserve a memory of the biological involvement by carrying strongly *negative* $\delta^{34}S$ (Berner 1970, 1984). We return to this later (Secular $\delta^{34}S$ trends in Eoarchean-Paleoarchean sulfides section), but it is well established that sediments deposited in Archean environments preserve $\delta^{34}S$ fractionations that are typically <20‰ (Sim et al. 2019), and for Eoarchean rocks of sedimentary protolith like BIFs, they are much less than that (≤10‰). This overall trend in mass-dependent sulfur isotopes is interpreted to mean that SO_4^{2-} concentrations in the Archean oceans were very low, and that MSR was unable to operate in the general absence of reactive sulfate (e.g., Fike et al. 2015).

The exception to sulfate-absent Archean oceans is the localized stabilization of SO_4^{2-} by fluids interacting with, for example, silicic magma chambers with associated caldera collapse and seawater incursions. These partially isolated environments will locally evolve highly oxidized (Scaillet et al. 1998) and volatile-rich saline fluids (Newton and Manning 2004) and the expulsion of these oxidized fluids stabilize SO_2. Confined to a regional volcano-sedimentary environment the SO_2 hydrolyzes reaction (Hattori and Cameron 1986):

$$4H_2O + 4SO_2 \leftrightarrow H_2S + 3H^+ + 3HSO_4^- \quad (9)$$

yields sulfate even without the free oxygen in the system, which then converts to (bi)sulfite (viz. Equation 8). Other products in this reaction are hydrogen sulfide and free hydrogen. For instance, microscopic sulfide (pyrite) grains co-exist with sulfates in the ca. 3.49 Ga barite (barium sulfate; $BaSO_4$) beds from the Dresser Formation, Warrawoona Group at North Pole in Western Australia (Philippot et al. 2007). These rocks formed at a time when there should have been no sulfate in ambient seawater. Underscoring how unusual these rocks are, is that sedimentary sulfates do not appear again in the rock record until about a billion years later in the Neoarchean (e.g. Zhelezinskaia et al. 2014).

Fractionations by MSR of the minor isotope ^{33}S have been recorded to yield relatively higher $^{33}S/^{32}S$ in product sulfide (e.g. Johnston et al. 2005; Ono et al. 2006). This process also, interestingly, results in small positive $\Delta^{33}S$ values. It is worth noting that this same process discriminates against ^{36}S, and thus to negative $\Delta^{36}S$ in the sulfide product relative to the starting values of the sulfate reactant. Johnston et al. (2007 and references therein) also reported $\Delta^{36}S/\Delta^{33}S$ of ~−6.9, with the magnitude of the changes in $\Delta^{33}S$ and $\Delta^{36}S$ observed to scale with degree of mass-dependent fractionation in $\delta^{34}S$.

Mineralogical aspects of microbial sulfur disproportionation

Microbial sulfur disproportionation (MSD) is a form of respiratory metabolism that uses sulfur as the electron acceptor in a series of redox reactions to generate ΔG°. Organisms metabolize sulfur intermediate compounds such as elemental sulfur (S^0 and sulfur polymers) and sulfite (SO_3^{2-}) to produce sulfide and sulfate as products (Bak and

Pfennig 1987; Canfield and Teske 1996; Canfield and Thamdrup 1994; Cypionka et al. 1998; Finster et al. 1998; Habicht et al. 1998; Rabus et al. 2013; Thamdrup et al. 1994). The disproportionation of inorganic sulfur intermediates can be done with our without free hydrogen present in the system. The general forms of these reactions are:

$$4S^0 + 4H_2O \rightarrow 3H_2S + SO_4^{2-} + 2H^+ \quad (10.1)$$

$$4SO_3^{2-} + 2H^+ \rightarrow H_2S + 2SO_4^{2-} \quad (10.2)$$

$$S_2O_3^{2-} + H_2O \rightarrow H_2S + SO_4^{2-} \quad (10.3)$$

Culture studies have shown that elemental sulfur disproportionation (Equation 10.1) typically concentrates ^{32}S in the sulfide product that in turn leads to mass-dependently fractionated negative $\delta^{34}S$ values between 5.5 and 11.3‰ (Canfield et al. 1998). In another culture study by Johnston et al. (2005), it was shown that the opposite sign can also occur, with positive fractionations in $\delta^{34}S$ up to ~4‰. Analyses of sulfite disproportionation reactions (Equation 10.2) also show that the product sulfide is depleted in ^{34}S and the sulfate product is enriched in ^{34}S (Habicht et al. 1998). Authenticated fractionations in sulfide $\delta^{34}S$ are between +20 and +45‰, and the sulfate shows $\delta^{34}S$ negative fractionation of −7 to −12‰ (Johnston et al. 2005). Very few data are currently available to allow us to confidently evaluate how $\Delta^{33}S$ values change in the sulfite disproportionation process, what does exist indicates that values of both products show *increases* in ^{33}S relative to the reactant SO_3^{2-}.

Post-depositional abiotic sulfur isotope fractionation processes

Thermochemical sulfate reduction (TSR) is thought to have been an active process within the Archean sulfur cycle even as it requires the presence of reactive sulfate (e.g. Jamieson et al. 2013). The TSR process may refer to either abiotic reduction of sulfate where Fe^{2+} acts as an electron donor (hereafter, TSR^1), or reduction of sulfate by organic carbon (TSR^2). These reactions happen at higher temperatures than MSR ('Atmospheric photochemistry and multiple sulfur isotopes' section), which has an optimal temperature range between ~20° and 40 °C (Canfield 2001; Jørgensen et al. 1990; Sageman et al. 1998). The two forms of TSR described above have been invoked to explain some features of the Archean sulfur cycle.

The TSR^1 process uses Fe^{2+} and free hydrogen H+ ('Environmental availability of free hydrogen' section) and occurs at temperatures of ~200°–350 °C (Trudinger et al. 1985), via:

$$8Fe_2^+ + 10H^+ + SO_4^{2-} \rightarrow 8Fe^{3+} + H_2S + 4H_2O \quad (11)$$

Isotope fractionation models (Janecky and Shanks 1988) show that the reaction leads to product sulfide concentrated in ^{34}S with positive fractionations of $\delta^{34}S \geq 5$‰. It is still unknown how this process (Equation 11) affects fractionation in the minor isotopes, if at all. In the geologic record, TSR^1 is usually recognized where sulfides that host negative $\Delta^{33}S$ values requiring the reduction of MIF sulfate to sulfide preserving the mass-independent signal, occurs within high-temperature chemical environments in the crust such as the volcanogenic massive sulfide (VMS) deposits (e.g. Bekker et al. 2009; Jamieson et al. 2006, 2013).

The TSR^2 involving organic matter—which itself is abundant in hydrogen—commonly takes place at temperatures of ~100°–140 °C and up to about 180 °C (Claypool and Mancini 1989; Machel 1998) in a mechanism resembling that in (Equations 9 and 10). Experiments have verified that the TSR^2 mechanism concentrates ^{32}S in the product sulfide and produces negative $\delta^{34}S$ fractionations between ~0 and 10‰ (Kiyosu 1980). Intriguingly, Watanabe et al. (2009) also showed that the product $\Delta^{33}S$ values are ~0.1−2.1‰ higher than that of the reactant sulfate.

Now that we have reviewed the general manner of microbial and abiotic sulfur isotopic fractionations, they can be placed in the context of the early evolution of the sulfur cycle and its bearing on record of microbial metabolic evolution in the Archean marine reservoirs.

Microbial sulfur reduction in the Archean marine system

Sulfur reservoirs in the marine system can be divided into three main components: Marine sediments, seafloor hydrothermal environments and seawater (aqueous) sulfate. Sulfide minerals can be found in rocks from each of these components in the geological. Such sulfides shown to carry *positive* $\Delta^{33}S$ values and relatively large *positive* or *negative* $\delta^{34}S$, and where these values deviate from the ARA in $\Delta^{33}S/\delta^{34}S$ space ('Atmospheric photochemistry and multiple sulfur isotopes' section), are typically ascribed to the action of MSD in the Archean (e.g. Wacey et al. 2010). This relationship in $\Delta^{33}S/\delta^{34}S$ space is illustrated in Figure 2(b) for the Paleoarchean sulfides with a noticeably wider range in $\delta^{34}S$ (inset) than in the preceding Eoarchean.

Authigenic sulfide mineral formation in Archean banded iron formations

Banded iron formations are characteristically laminated Fe-rich (~20–40 wt.% Fe) siliceous (~40–50 wt.% SiO_2) sedimentary rocks that formed extensively in the oceans throughout the first 2 billion years of Earth history (James 1954). The formation of BIF was perhaps modulated by life (Kappler et al. 2005), which would qualify the rock type as a biomarker. At the time of sedimentation, the primary Fe-mineralogy of the BIFs included hydrated ferric oxyhydroxides ($Fe^{3+}O(OH)\cdot nH_2O$), the serpentine-group mineral greenalite ($(Fe^{2+},Fe^{3+})_{2-3}Si_2O_5(OH)_4$), and the ferrous-carbonate mineral siderite ($Fe^{2+}CO_3^{2-}$) (Han 1966). Subordinate primary minerals included sulfide, (basic calcium) phosphate, and organic matter (Klein 2005). It is also probable that the oceans at that time were enriched in dissolved silica (Konhauser et al. 2007) and under such conditions the precipitation of amorphous silica can take place directly on the sea floor out of solution. Consequently, this

would add silica to the list of primary minerals in BIFs (Krapež et al. 2003).

Depending on the degree of metamorphism, the most common sulfide minerals present in BIF are pyrite (FeS_2; Figures 1 and 3) and its high-temperature (metamorphic) polymorph pyrrhotite ($Fe_{1-x}S$ [where, $x = 0$–0.2]).

As previously discussed ('Archean MIF sulfur aerosols, atmosphere transparency, low pO_2, and scattering' section) characteristic *positive* $\Delta^{33}S$ and *negative* $\Delta^{36}S$ values of Archean sulfides are indicative of the reduced, MIF elemental sulfur aerosols that were transported to the oceans, converted to sulfide and subsequently preserved in sediment (e.g. Izon et al. 2015).

Our focus is mainly on the geological record of BIFs, because they are the most abundant (preserved) of all Eo- to Paleoarchean sediments (Klein 2005). Yet, how were the MIF elemental sulfur aerosols converted to sulfide and incorporated into sulfide minerals? The possible mechanism depends on whether the mechanism was biologically modulated or not.

A plausible path for this process is via H_2S production from S^0 in MSD (Equation 8.1), followed by what has been proposed as a direct reaction of product sulfide with abundant $[Fe^{2+}]_{aq}$ in the Archean oceans (Holland 1973, 1984), as in:

$$Fe^{2+} + S_2{}^{2-} \rightarrow FeS_2 \quad (12)$$

Note that Canfield and Thamdrup (1996), Pyzik and Sommer (1981), and Schoonen and Barnes (1991) provide important caveats about sulfide saturation in the simple scenario (Equation 10).

Alternatively, elemental sulfur aerosols (S^0, S_{n+1}, cyclic S_8, polymeric $S_x{}^{2-}$) can react *directly* with ferro-ferric oxy-hydroxides; these were abundant in solution in the Archean oceans (e.g., Arrhenius et al. 1993). The relevant reaction is:

$$5S^0 + Fe_3(OH)_8 \rightarrow 3FeS + 2SO_4{}^{2-} + 8H^+. \quad (13)$$

Here, the reactivity of aqueous $Fe_3(OH)_8$ with elemental sulfur produces hydrogen. The compound $Fe_3(OH)_8$ is a mixed-valence iron oxy-hydroxide dubbed ferrosic hydroxide (Arden, 1950); it is an unstable precursor to magnetite in ferruginous sediments. Ferrosic hydroxide belongs to a mineralogical family of mixed valence compounds termed *Green Rusts* which have general compositions that vary from $Fe_2(OH)_5$ (Trolard et al. 1997) to $(Fe^{2+}{}_{(1-x)}\ Fe^{3+}{}_x - (OH)_2)^{x+}$ $(x/nA^{n-}\ m/n\mathrm{H2O})^{x-}$ (Génin et al. 1998), where A can be substituted by the anions OH^-, Cl^-, $CO_3{}^{2-}$ or $SO_4{}^{2-}$. Several studies have implicated the *Green Rust* precursor minerals as the feed stocks of the magnetite found in the Archean BIFs (Arrhenius 2003; Halevy et al. 2017; Kuma et al. 1989).

A further pyrite-forming pathway to consider is the polysulfide reaction wherein pentasulfide ($S_5{}^{2-}$) reacts with FeS to give FeS_2 and S_8 (Kafantaris and Druschel 2020; Rickard and Luther, 2007). Polysulfides ($S_x{}^{2-}$; x = 2 to 8 in natural systems; Kamyshny et al. 2003) in our case come into play via the abundant S^0 aerosols known to exist and traced by MIF from atmospheric reactions on the early Earth ('Atmospheric photochemistry and multiple sulfur isotopes' section). Intriguingly, chain-length distribution of the S^0 aerosols in aqueous systems is determined by disproportionation reactions, principally:

$$S_4{}^{2-} + 1/4\ H_2O \leftrightarrow 3/4\ S_5{}^{2-} + 1/4\ OH^- + 1/4\ HS^- \quad (14)$$

Whereupon the pentasulfide reacts to form pyrite.

Secular $\delta^{34}S$ trends in Eoarchean–Paleoarchean sulfides

Notably for our work, the geological record of $\delta^{34}S$ fractionations for Eoarchean sediments in Figure 2(a) (see inset) shows that this mass-dependent process was subdued; Eoarchean sulfur isotopes preserve small $\delta^{34}S$ fractionation values ascribable either to abiotic processes ('Post-depositional abiotic sulfur isotope fractionation processes' section) or perhaps to a simple form of elemental sulfur reduction (Kaplan and Rittenberg 1964). The earliest evidence for MSD as reported in Philippot et al. (2007) and Mojzsis (2007), takes the form of pyrite with *positive* $\Delta^{33}S$ values and where these values begin to significantly deviate from the ARA in $\Delta^{33}S/\delta^{34}S$ space is in the Paleoarchean record and afterwards (Figures 2(b, c); insets). By Neoarchean time (Figure 2(d), inset) the sulfur isotopes are strongly mass-dependently fractionated.

Eoarchean sulfides are characterized by a very narrow range of $\delta^{34}S$ values (inset, Figure 2(a)) that points to minimal fractionation between sulfate and sulfide (Figure 4) with the important caveat that no data are thus far available from the paired sulfate-sulfide samples necessary to constrain this fractionation (Fike et al. 2006, 2015; Fike and Grotzinger 2008; Gill et al. 2011). Geochemical studies and laboratory microbial culture work to explore the impact of sulfate concentration on fractionation during microbial sulfate reduction, show that such reduced $\delta^{34}S$ fractionations in sedimentary sulfur minerals is evidence for sulfate abundances sufficiently low (<200 μM) to inhibit any fractionation during that time (Habicht et al. 2002). Other results (Crowe et al. 2014; Zhelezinskaia et al. 2014) suggest even lower ambient sulfate levels (<10 μM) in the early Archean ('Authigenic sulfide mineral formation in Archean banded iron formations' section).

Furthermore, high-resolution spatial analysis by secondary ion mass spectrometry (SIMS; ion microprobe) of Archean pyrites documents higher fractionations than are apparent from bulk $\delta^{34}S$ pyrites (Mojzsis et al. 2003; Kamber and Whitehouse 2006). These preserved micrometer-scale $\delta^{34}S$ differences occur in pyrites that also preserve mass-independent signatures. These data confirm that the variable fractionations in $\delta^{34}S/\Delta^{33}S$ within Eoarchean to Paleoarchean sedimentary pyrites are primary and not the result of later-stage overprinting (Watson et al. 2009).

Evolution of biological sulfur cycling on the eoarchean to paleoarchean earth

Next, we now explore how the genes involved in sulfur metabolism may have evolved on the Eoarchean to Paleoarchean/Mesoarchean Earth to account for the observed trends in the multiple sulfur isotope data.

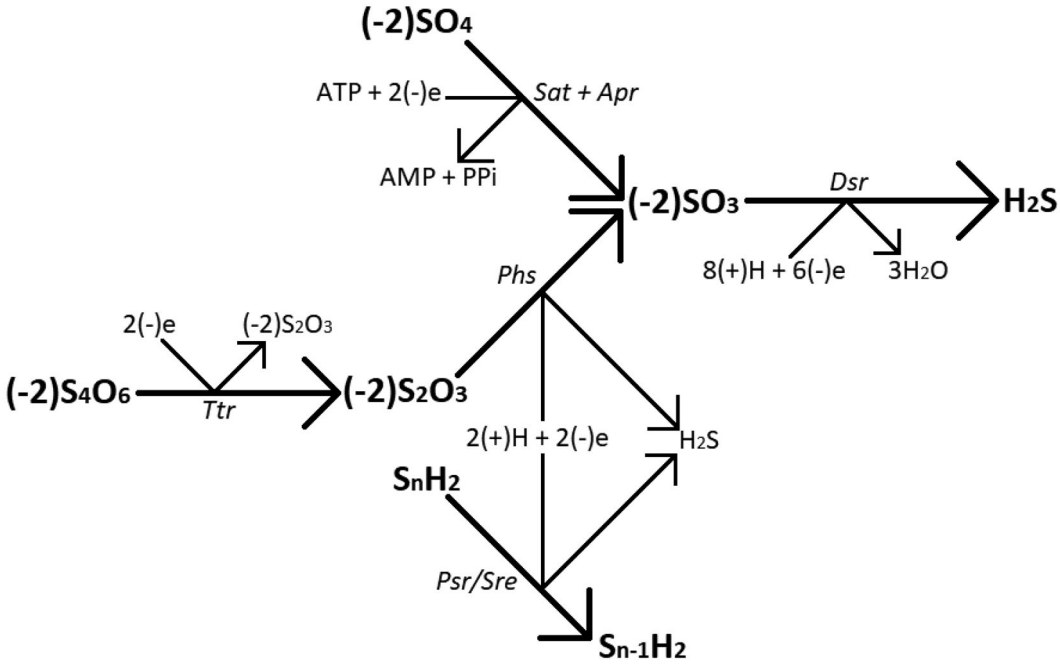

Figure 4. The major dissimilatory sulfur reduction pathways (modified from Rabus et al. 2013).

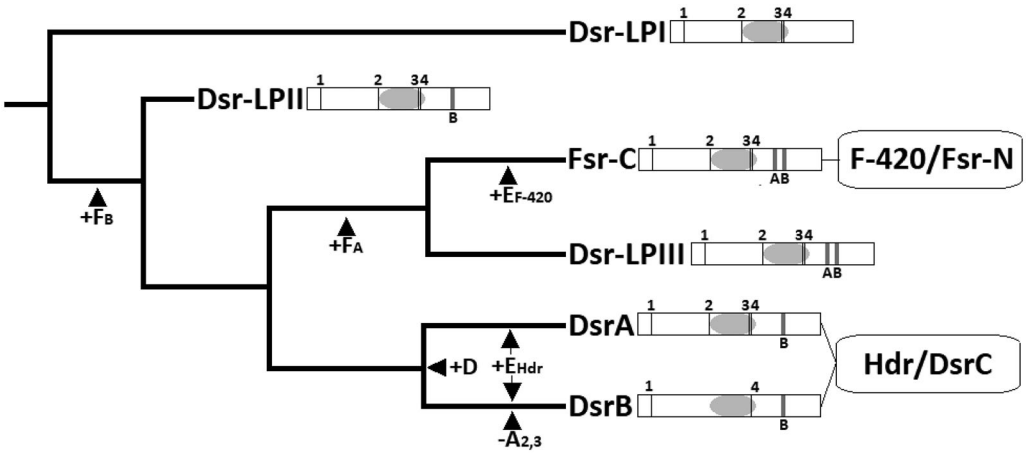

Figure 5. Position of the *DsrA* and *DsrB* subunits within the phylogeny of *Dsr*-like proteins in methanogens and the corresponding gene annotations. Black bands represent *Arg/Lys* binding sites (numbered C to N) while gray bands represent iron-sulfur clusters. F, A, D and E represent the insertion (+) or deletion (−) of an iron–sulfur cluster, *Arg/Lys* binding site, gene duplication or coupling of an ETC associated enzyme (adapted from Susanti and Mukhopadhyay 2012; Grein et al. 2013).

Life and the first 'hydrogen economy'

In the contemporary oceans, MSR is responsible for ~50% of the remineralization of all organic matter. In this pathway ('Atmospheric photochemistry and multiple sulfur isotopes' section), sulfate is taken up and reacted with ATP via sulfate adenylate transferase (*Sat*) to form APS (Figure 5). Then, an Andenlyl-sulfate reductase (*Apr)* enzyme cleaves the bond between the phosphate and sulfate group to form sulfite. This is then reduced to sulfide via a dissimilatory sulfite reductase (*Dsr*) located at the end of an electron transport chain; the electrons either being derived from an organic molecule or hydrogen (Grein et al. 2013). The enzymes that carry out the reactions are homologs, even if there are many alternative pathways oxidation usually takes (Weissgerber et al. 2014). Other forms of sulfur can also be utilized.

Elemental sulfur, thiosulfate ($S_2O_3^{2-}$) and tetrathionate ($S_4O_6^{2-}$) can ultimately be reduced to sulfide via polysulfide/sulfur (*Psr/Sre*), thiosulfate (*Phs*), and tetrathionate (*Ttr*) reductases in sulfur reducing microbes (Laska et al. 2003), and oxidized to sulfate using *Sox* enzymes in sulfur oxidizers (Figure 6). Furthermore, sulfides can be oxidized to elemental sulfur in sulfur oxidizers via sulfide quinone reductases (Gregersen et al. 2011). Finally, elemental sulfur and thiosulfate can be disproportionated by sulfate reducers using sulfur oxidoreductases (Thamdrup et al. 1993).

Eoarchean alkaline hydrothermal vents as a waystation for early life

The microbial community that composed LUCA may have included a hydrogenotrophic acetogen with a primordial

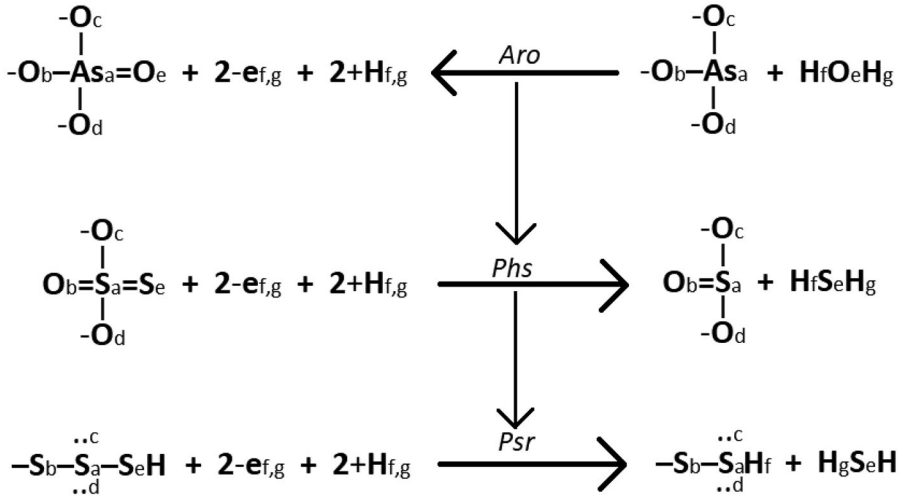

Figure 6. A proposed scenario for the evolution of the *Phs* and *Pse/Sre* enzymes. Horizontal arrows indicate the direction in which the reaction occurs whereas subscript letters by the atoms in each molecule show where a homologous site in each enzyme would interact with the products and reactants (modified from Duval et al. 2008).

metabolism utilizing the Wood–Ljungdahl pathway (Russell and Martin 2004). To better understand the nature of this early biosphere, modern analogue environments conventionally serve as a guide. Enzymes involved in the W–L pathway have many cofactors that resemble minerals involved in the abiotic synthesis of organic molecules in alkaline hydrothermal systems (Russell et al. 2013). We now explore these chemically dynamic environments as a *salle d'attente* for emergent life.

We have reiterated the case that at least at some transitional stage Earth's Eoarchean–Paleoarchean biosphere included a biome that resided at alkaline hydrothermal vent systems. The deepest-rooted forms of metabolism have a similar series of reactions that are identified to occur in mafic (alkaline) hydrothermal vents, whether on the seafloor or the shallow sub-surface. It is interesting to note that even on the contemporary Earth, a combination of biotic and abiotic carbon fixation reactions can take place within these environments (e.g. Martin and Russell 2007). Further, the presumed biogenic carbonaceous materials measured in sediments from such environments have a $\delta^{13}C$ range of -28.9 to $-21.5‰$, whereas postulated abiogenic carbon varies from -15 to $-9‰$ (Proskurowski et al. 2008); this range is similar to that observed in Eoarchean rocks ascribable to evidence of past biological activity (Havig et al. 2017; Papineau et al. 2010). As we argue later, by approximately Paleoarchean time, data from the rock record seem to indicate that life went from exclusive hydrogenotrophic carbonate reduction to a variety of metabolisms including methanogenesis (e.g. Ueno et al. 2006), photosynthesis (e.g., Olson 2006) and respiration (e.g. Bontognali et al. 2012). This evolution toward metabolic complexity is the natural consequence of life's dependence on non-equilibrium electron transfers (Falkowski 2006).

If alkaline hydrothermal vents were a stepping stone for early life (see Martin 2017 for a summary), we may inquire what happened as more metabolic pathways emerged in this environment? Biosynthetic pathways that would have produced materials needed for metabolism (such as nucleic acids and enzyme co-factors) were at first synthesized via abiotic processes (e.g. in the serpentinization environment) and inherited by the earliest organisms (Wang et al. 2014). Such early emergent biosynthetic pathways ought to include those involved in ever more sophisticated amino and nucleic acid biosynthesis, which would lead to an ever greater chemical distinction between the portions of the hydrothermal crucible where biogenic and abiogenic carbon reduction took place (e.g. Martin and Russell 2007). Once hydrogenotrophic acetogenesis was firmly established by this nascent biome (see, for example, Figure 1 of Martin 2017), it set the state for diversification into methanogenesis; this increased the total energy obtained from carbonate reduction and fermentative heterotrophs which allowed organisms to derive energy from previously reduced carbon (Schönheit et al. 2016). Although the evolution of biosynthetic pathways would have allowed life to survive throughout an alkaline vent, we argue that it would still be limited to near-vent niches for reliable access to the mineral precursors of the functional groups used to catalyze metabolism. Only after gaining the ability to synthesize these cofactors from more and more simple starting materials, could organisms venture forth beyond the hydrothermal cradle into the surrounding marine habitats. That is, if the required raw materials, hydrogen and inorganic carbon, were present for a relocation (Holliday et al. 2007).

Environmental availability of free hydrogen

A number of natural mechanisms are available to provide crustal H_2 to the environment (e.g. Morita 1999) (Equations 1, 9, 10, 13), but an important caveat to these various sources is that the hydrogen must be at least at the minimum abundance levels required for H_2-dependent growth (Schink 1997; Thauer et al. 2008). This is a challenge because hydrogen gas in the environment is ephemeral with very fast diffusion times. Free hydrogen can be formed in relatively low oxygen fugacity reactions between dissolved gases in the system C–H–O–S in magmas, especially in those with basaltic

affinities that continuously form and sustain hydrothermal vents; by thermal decomposition of organic matter and CH_4 to C^0 and H_2 at temperatures around 600 °C; via reaction between CO_2, H_2O, and CH_4 at elevated temperatures in the vapor phase; from radiolysis of water by U and Th, and their radioactive (intermediate) daughters, and potassium-40; catalysis of silicates under stress in the presence of water; hydrolysis of ferrous minerals in ultramafic rocks (peridotite, komatiite); and, mantle exhalations via volcanic or passive crustal out-gassing. These various sources of hydrogen are frequently misconstrued to mean that there is no strong limitation to free hydrogen availability for metabolism. Of the endogenous sources, H_2 from vents and the serpentinization process is the most important. Methanogens and acetogens and H_2-dependent microbes in general need on the order of 1–10 Pa H_2 for the metabolic reaction to being exergonic. It is for this reason they grow near serpentinizing systems, or occur together with H_2-producing fermenters. To underscore this point, it is not enough that free hydrogen can be made at the crust-hydrosphere interface, it must be an adequate abundance to be useful (e.g. Orsi et al. 2020).

Once a dependable capacity to produce the organic and inorganic molecules could be found to sustain cellular metabolism away from a reliable source of H_2 and mineral precursors at alkaline hydrothermal vents, later microbial life was no longer confined to these environments. Yet, and interesting challenge for early life arises: sulfur oxides (SO_n; $n = 1, 2, 3$) released by volcanic and passive outgassing in active hydrothermal regions quickly react with water to form bisulfite (HSO_3^-) and thence sulfite (SO_3^{2-}) as in:

$$SO_2 + H_2O \leftrightarrow HSO_3^- + H^+ \quad (15.1)$$

$$HSO_3^- \rightarrow SO_3^{2-} + H^+. \quad (15.2)$$

The product (Equation 15.2) can be oxidized further to form sulfate (SO_4^{2-}), or sulfuric cid (H_2SO_4) depending on the pH (e.g. Ranjan et al. 2018). In the absence of available oxygen to deep Eoarchean-Paleoarchean hydrothermal environments, the bulk of the sulfur (Rimmer and Shorttle 2019) will be in the form of bisulfite (HSO_3^-) and hydrogen sulfide (HS^-). Sulfite is highly reactive and requires detoxification by microbes ('Sulfite detoxification' section).

Selective pressures on the early biochemical evolution of sulfur metabolism

The ability to metabolize elemental sulfur would not have emerged *de novo*; it must have evolved from an existing enzyme that was already integrated into a metabolic system (Duval et al. 2008). To understand why it was delayed until the Paleoarchean, we must understand what metabolic systems and what environmental conditions were present to account for this delay. While data indicate that ESR was operative by 3.5 Ga (Philippot et al. 2007), molecular evidence is at odds with this being the oldest form of sulfur metabolism; other forms of sulfur metabolism were there first (Duval et al. 2008). Phylogenetic evidence shows that some of the genes involved in respiratory sulfur metabolism were present in the LUCA microbial community (Heinzinger et al. 1995).

We now examine the sulfur metabolic processes in methanogens and acetogens to understand this further, and explore how early life was forced to cope with toxic sulfite.

Sulfite detoxification

In methanogens that inhabit sulfur-rich hydrothermal environments (e.g. Takai et al. 2004), a class of enzymes is present that closely resemble *Dsr* (Life and the first 'hydrogen economy' section) which are used to detoxify sulfite by reducing it to sulfide. The first *Dsr-LP* to evolve was cytoplasmic and obtained electrons from intracelluar Fe–S clusters which themselves would have obtained electrons from an unknown enzyme. A later variety integrated the Fe–S clusters within the enzyme which allowed the *Dsr-LP* to obtain electrons directly from it, facilitating greater reaction rates (Susanti and Mukhopadhyay 2012). After a duplication (forming the A and B subunits; Dhillon et al. 2005), molecular analysis shows that the *DsrM* complex which links the *DsrAB* to the electron transport chain is homologous to the hetero-disulfide reductase enzymes (E subunit) of methanogens. This is also involved in the electron transport chain, which implies that the binding of the ancestral *DsrAB* complex to an *HdrE* linked it to the central energy metabolism and allowed to act as an electron acceptor in the earliest form of respiration (Grein et al. 2013). A variety of *Dsr-LP* known as *Fsr* appears to have been convergently coupled with the *F420-H2 Dehydrogenase* enzyme. A variety of the derivation of *Dsr* from an enzyme utilized by methanogens to detoxify sulfite suggests to us that sulfur metabolism may have started out at hydrothermal vents perhaps evolved from a carbonate-reducing metabolism.

Abundant sulfite in the environment provided at least a mild selective pressure on methanogens to detoxify it. Initially, early *Dsr-LP* would have had low reaction rates but with the incorporation of sirohemes, electron transfer efficiency increased, allowing it to reduce sulfite at an increased rate (Susanti and Mukhopadhyay 2012) and inhabit deeper parts of the hydrothermal vent system with greater concentrations of H_2 present (McCollum 2007). As the organisms colonized microhabitats with ever higher concentrations of sulfite, the selective pressure to detoxify it may have driven the coupling of the *Dsr-LP* to the central energy metabolism, and thus to respiration (Grein et al. 2013).

Among the many forms of sulfur respiration, sulfite reduction has some inherent limitations due to the toxicity of the substrate (Simon and Kroneck 2013). By allowing for greater metabolic rates, this would have favored the evolution of sulfur respiration systems that could reduce other less-toxic oxidized sulfur compounds. Although organisms that had evolved the capacity to reduce other sulfur sources would still have inhabited an environment where sulfite was present, the uptake of sulfite into the cytoplasm where it would do the most harm would no longer be required to carry out respiration (Dudley and Frost 1994). While sulfate was present at trace amounts, hydrolysis reactions between

sulfur dioxide and calcium oxide and the reactions discussed above could also have produced sulfate in Hadean-Archean volcanic vents (Arndt and Nisbet 2012) and when alkaline conditions are present, sulfides readily react with water to form thiosulfate (Gartman and Luther 2013). For more about reactions that yield sulfate in the pre-GOE Earth, we refer the reader to Mineralogical aspects of microbial 'sulfate reduction' section.

The competing back reactions to elemental sulfur can occur with oxidation of hydrogen sulfide (Luther et al. 2011) and the acid dissociation of thiosulfate (Xu et al. 1998) and polysulfide (Luther 1990).

Rise of sulfate, thiosulfate, tetrathionate, and elemental sulfur metabolisms

After the first form of sulfur respiration evolved, other styles would follow suit including the ability to utilize sulfate, thiosulfate, tetrathionate, and elemental sulfur/polysulfides (e.g., Duval et al. 2008). The latter three of these sulfur species are reduced by enzymes in the molybdopterin superfamily. Of the genes in this family likely evolved from an arsenite oxidase (*Aro*) enzyme present since before the community of LUCA (Lebrun et al. 2003). Of the sulfur species metabolized by genes in this family, the molecular structure of thiosulfate most closely resembles arsenate. Consequently, one likely scenario for the incorporation of it in sulfur metabolism is that an ancient *Aro* enzyme became attached to the end of the electron transfer chain causing it to reduce the substrate as opposed to oxidizing it and reversing the reaction (Heinzinger et al. 1995) and bound thiosulfate to the active site. The modern *Phs* is capable of reducing compounds with a similar molecular structure to thiosulfate such as perchlorate and may be able to reduce arsenate itself (Duval et al. 2008). Due to high sequence similarity, *Phs* and *Psr*/*Sre* are often not distinguished from one another on phylogenies, but Melton et al. (2016) showed that when differentiated it appears that *Psr* was monophyletic while *Phs* was paraphyletic. This reinforces the notion that *Phs* represents the primitive character state of the sulfur metabolizing enzymes in the molybdopterin family. Furthermore, the *Phs*/16srDNA phylogenies are congruent across archaea and bacteria indicating that this gene was also present at LUCA (Duval et al. 2008).

Presently, sulfate is most widely used in sulfur-based respiration owing to its abundance in seawater. Yet, the utilization of sulfate required the evolution of two other enzymes: sulfate adenylyltransferase (*Sat*) and adenylylsulfate reductase (*Apr*). The *Sat* enzyme is a transferase related to kinases (Segel et al. 1987) whereas *Apr* is a reductase enzyme distantly related to other flavoproteins with a high structural but low sequence similarity (Grein et al. 2013). The phylogeny of *Apr* has a root is between sulfur-reducing Archaea and group I sulfur-oxidizing bacteria with sulfur-oxidizing group II branching off from the sulfate reducers (Meyer and Kuever 2007). When sulfur-oxidizing and sulfur-reducing *Dsr* genes are placed on a phylogeny, the branches by the root are comprised of sulfur reducers with sulfur-oxidizing bacteria branching off later (Müller et al. 2015). The combined *Dsr* and *Apr* gene phylogeny indicates that shortly after the ability to reduce sulfate had evolved in a stem group Archaeon, stem group Bacteria acquired *Sat* and *Apr* via horizontal gene transfer where the pathway was reversed (Hipp et al. 1998).

Arrival of photothiotrophy

A proposed mechanism for this reversal is when a photon struck a heme group in the electron transport chain provided an excess of energy (a product), that reversed the direction of the reaction (Figure 7). If this interpretation is correct, the heme group served as the precursor of the first photosynthetic pigments (bacteriochlorophyll utilized by photothiotrophs is structurally intermediate between tetrapyrroles and chlorophyll) while the protein in which it resides served as the ancestral photosystem (Martin et al. 2018). The advent of photosynthesis forever altered the stoichiometry of the global biosphere (e.g. Falkowski and Raven 2007); this newly emergent pathway would have swamped the environment with an *abundant electron acceptor*, organic carbon.

Discussion

Elemental sulfur reduction has been shown to be the oldest form of sulfur respiration for which isotopic evidence exists, yet the molecular evidence is at odds with this being the first sulfur metabolic style. Given that *Phs* occupies the branches at the root of the *Psr*/*Phs* gene tree (Melton et al. 2016) and has a substrate with greater similarity to that of *Aro* (Duval et al. 2008), thiosulfate reduction likely preceded it. Furthermore, *Phs* produces sulfite as a product (Rabus et al. 2013) which would have quickly built up to toxic levels in the cell if *Dsr* had not been present (Simon and Kroneck 2013) indicating that sulfite reduction had to precede elemental sulfur reduction. While the incorporation of the *Phs* into dissimilatory sulfur metabolism gave early respiratory organisms the precursor of the enzyme used to metabolize elemental sulfur, it was likely the incorporation of the *Sat* and *Apr* enzyme (more specifically, the pathway reversal that followed; Hipp et al. 1998) that provided the ultimate evolutionary incentive to utilize it.

Straying from the alkaline vent

Primary productivity in contemporary hydrothermal vents is usually carbon (electron acceptor) limited (Proskurowski et al. 2008), which means that early life forms would have competed for this resource (McCollum 2007). It is interesting to note that high-temperature ultra-magnesian systems—where H_2 is most abundant—tend to have low oxygen fugacity and consequently relatively higher H_2S/SO_2 values (Hoshyaripour et al. 2012). Arguments have been presented that such vent chemistries were relatively commonplace on the Hadean–Eoarchean Earth (Arndt and Nisbet 2012). Any adaptation that allowed the first organisms to synthesize the cofactors from more simple starting materials

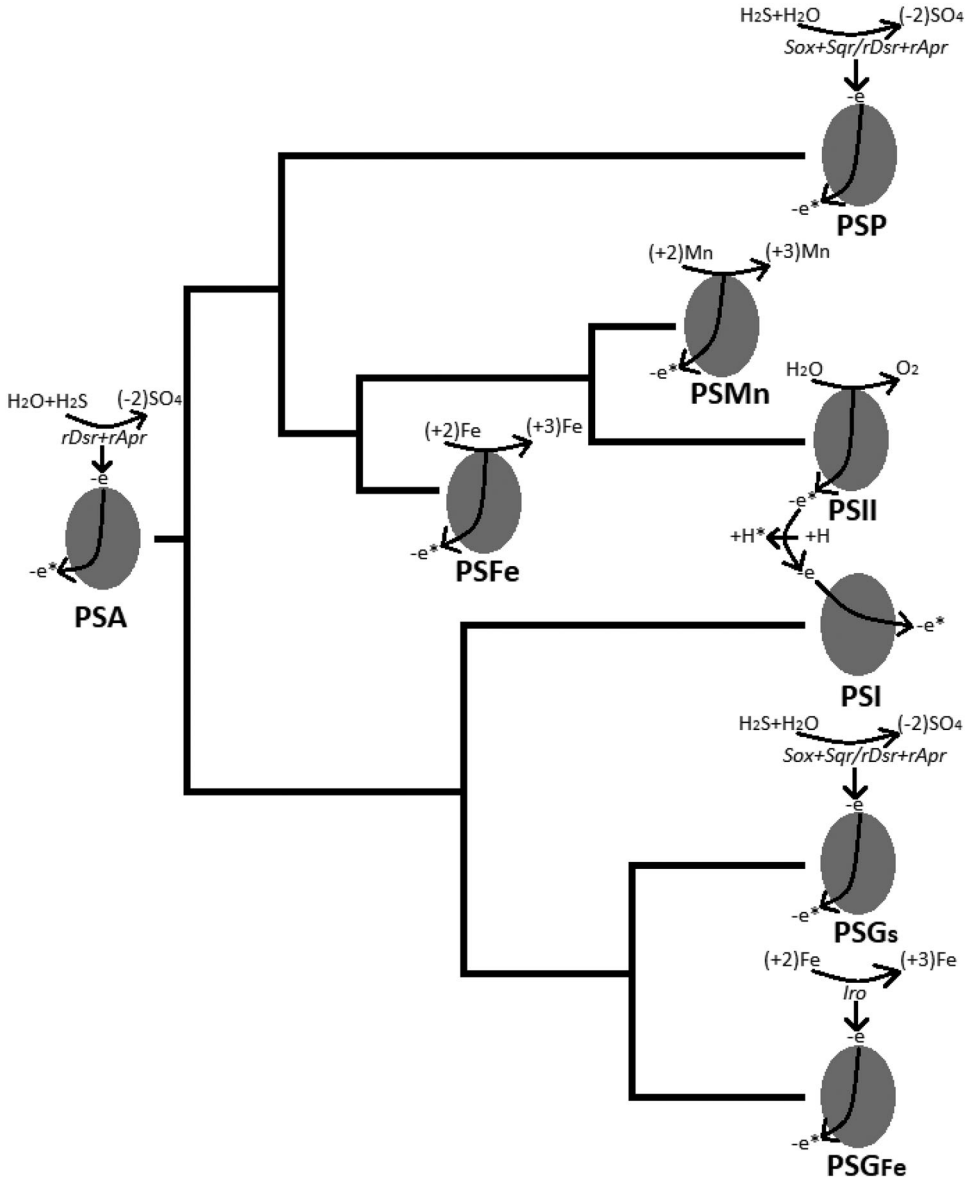

Figure 7. Possible phylogeny of the photosystems used in photosynthesis and the reaction each catalyzes with an asterisk by an electron or proton indicating that it is in a high energy state. PSA = ancestral photosystem, PSII = photosystem II, PSI = photosystem I, PSP = purple sulfur bacteria photosystem, PSGS = greens sulfur bacteria (sulfur-oxidizing) photosystem, PSGFe = greens sulfur bacteria (iron-oxidizing) photosystem, PSFe = iron-oxidizing photosystem, PSMn = manganese-oxidizing photosystem (modified from Martin et al. 2018; Xiong 2006).

gave them the new ability to carry out carbon reduction in a wider array of microhabitats in the marine realm (Sojo et al. 2016). Once this was threshold was breached, colonization of the water column became possible.

With a lower organic carbon to carbonate ratio than the modern biosphere (1:9 as opposed to 1:5), the Eoarchean biosphere was both puny and less productive (Schidlowski et al. 1975; Schidlowski 1982). While it has been speculated that this was due to a lower supply of nutrients (e.g. Sleep and Bird 2007), estimates of productivity have indicated that the ancient biosphere was more specifically limited by the supply of electron donors (Ward et al. 2019). In ultramafic hydrothermal systems such as Lost City (Kelley et al. 2001), primary productivity is *electron acceptor limited*. At the periphery of the vent, however, life encountered an ocean rich in bicarbonate yet relatively poor in free hydrogen. This reverses the selective pressures on an Eoarchean biosphere that strayed from the hydrothermal vents to one that goes from electron acceptor- to donor-limited (Ward et al. 2019). The evolution of heterotrophic processes and methanogenesis (Martin and Sousa 2015) would have also allowed those organisms to remineralize organic carbon produced within and around the vent to methane and carbon dioxide (Whiticar and Faber 1986).

With the first branching of the *Apr* phylogeny being between sulfur-reducing and oxidizing organisms, it is likely that the ability to oxidize sulfur began shortly after the enzyme was incorporated into sulfur metabolism (Meyer and Kuever 2007). If sulfur oxidation originated as a result of a reversal in the sulfur respiration pathway (Hipp et al.

1997), such a switch is unlikely to have occurred when *Dsr* was the only enzyme present due to the production of toxic sulfite (Simon and Kroneck 2013).

Sulfur and the dawn of photothiotrophy

Before photosynthesis, MSR near volcanic vents would have been limited primarily by the supply of electron donors in the system due to the high ratio of sulfur dioxide derivatives to molecular hydrogen (e.g. Nakamura and Takai 2014), except in the cases of the hottest, most magnesian and H_2-rich hydrothermal centers ('Straying from the alkaline vent' section). This would have held true especially in the cooler more oxidized periphery of the vent community because the concentration of oxidized sulfur species exceeds that of hydrogen (free or bound to a carbon) and any external source of carbon would have been fermented by methanogenesis (King 1984; Ueno et al. 2006). While most volcanic vents have a greater concentration of sulfate and sulfite than hydrogen, sulfides still dominate (Nakamura and Takai 2014). This would result in sulfur oxidation outpacing respiration if we assume that both are only using sulfur electron donors/acceptors that are derived from the vents (McCollum 2000).

We propose that the increased abundance of organic carbon as an electron donor provided an electron donor for elemental sulfur reduction to account for its utilization by about 3.5 Ga based on the data shown in Figure 2 which shows a marked increase in mass-dependent fractionation. Due to the high sequence similarity between the *Psr* and *Phs* genes, relatively few mutations would have had to occur to allow the gene to reduce elemental sulfur (Duval et al. 2008), indicating that this transition could have taken place rapidly should selective pressures arise to motivate it. While the abundance of electron donors may explain why elemental sulfur was used as an electron acceptor, it should not be forgotten that elemental sulfur is in an intermediate oxidation state (Gregersen et al. 2011).

Elemental sulfur reduction appears in the paleoarchean as opposed to other S^0 pathways

The isotopic evidence in Figure 2 hints that biological S^0 reduction began in the Paleoarchean, but are other forms of sulfur metabolism not observed at or before this time in the geochemical record? It is likely because those pathways had not yet evolved. Schut et al. (2013) argue that the sulfur reduction systems of Archaea evolved from fermentative H_2 production. If, as suggested by Martin (2017) and Sousa et al. (2018) the fermentative reduction of sulfur was active in the Paleoarchean, and cytochrome-dependent sulfur reduction came later, then we may be seeing evidence of this evolutionary innovation in the isotopic geochemistry.

Sulfur disproportionating organisms use sulfur oxidoreductase enzymes to metabolize elemental sulfur and it is not known how this enzyme is related to others (Urich et al. 2004). This makes it difficult to understand the circumstances under which it evolved but it is known that the disproportionation of elemental sulfur must be coupled with the reduction of ferric iron to be exergonic (Thamdrup et al. 1993). The magnetite in the oldest banded iron-formations is diagenetic from *Green Rust* (Mineralogical aspects of microbial 'sulfate reduction' section) which means that the supply of ferric iron would be limited by solubility, thus removing the evolutionary pressure to metabolize elemental sulfur.

It is documented (Franz et al. 2007) that some contemporary photothiotroph strains such as *Allochromatium vinosum* use elemental sulfur, indeed all sulfur-oxidizing microbes use elemental sulfur as an intermediate in sulfur oxidation (Gregersen et al. 2011). Yet, as shown in Secular $\delta^{34}S$ trends in Eoarchean-Paleoarchean sulfides section the lack of isotopic evidence for elemental sulfur oxidation to sulfate until the Neoarchean as indicated by the presence of sulfates with positive $\Delta^{33}S$ values (Paris et al. 2014)suggests to us that the ability to oxidize elemental sulfur had not evolved until that time even if the genes were present. With the exception of a *Psr*-like gene used to oxidize sulfate to sulfite in one OTU of purple sulfur bacteria, utilizing the *Dsr*, *Apr* and *Sat* genes while lacking the *Phs* and *Psr* enzymes, makes it seem likely that the latter two were not present in first sulfur-oxidizing microbes if the pathway ended up becoming reversed (Hipp et al. 1998).

Contemporary sulfur oxidizers use the *Sox* multi-enzyme complex which is in the cytochrome oxidoreductase gene family, implying that unlike sulfur reducers, early sulfur oxidizers did not have an enzyme already used in sulfur metabolism that could be converted into one that oxidized elemental sulfur (Ghosh et al. 2009). Furthermore, while sulfur reducers can use sulfate bound in barite (albeit at an attenuated rate) , sulfur oxidizers cannot do the same with sulfide bound in pyrite (Rawlings et al. 1999).

Sulfur reducers living in the periphery of a volcanic vent would face electron acceptor limitation over a wide range while photothiotrophs would have a narrow band of limitation around the periphery before being subjected to complete inhibition (Rawlings et al. 1999), restricting how many photosynthetic organisms faced electron donor limitation. The first photosynthetic organisms may not have used another sulfur source as an electron donor, or they used a different element entirely (Martin et al. 2018).

Conclusions

We show that the expansion of microbial control of the sulfur cycle from the earliest vestiges of the geologic record can be traced by sulfur isotope geochemistry (e.g. Thiemens and Lin 2019). Prior to the evolution of the contemporary array of sophisticated sulfur metabolic styles, Earth's earliest biosphere was meager, perhaps powered mostly by the reduction of carbonates using hydrogen as the electron donor where it was locally over-abundant (e.g. Martin 2016; Sleep and Bird 2007). We hypothesize that a waystation for the early biosphere was in hydrogen-rich alkaline hydrothermal vents.

We further speculate that the springboard to novel sulfur-based metabolisms at the Eoarchean to Paleoarchean transition (i.e. from ca. 3.85 to 3.5 Ga) came about from the sulfur-reducing genes of a precursor variety associated with dissimilatory carbon metabolism. This would place the timing of the colonization of the volcanic vent environments to the end of the Eoarchean. This idea comports well with the notion of an early microbial biosphere powered at some stage primarily by the reduction and fermentation of carbon (Schönheit et al. 2016; Weiss et al. 2016). This evolutionary innovation was then followed by the ability to utilize thiosulfate (Duval et al. 2008) and sulfate (Meyer and Kuever 2007) as electron acceptors. If the systems that the first sulfur-reducing microbes inhabited were electron donor limited, then why did these organisms evolve the ability to utilize other sulfur sources?

If early sulfur reducers could utilize other sources of sulfur then the quantity of sulfite uptake required to sustain respiratory processes would decrease, thus giving these organisms an advantage (Widdel and Pfennig 1981). After *Phs* had evolved from an *Aro*, the earliest sulfur reducers possessed a gene that with few modifications that could use elemental sulfur as an electron acceptor (Duval et al. 2008). An evolutionary pressure would have to be present to induce this alteration.

We also propose that the excitation of electrons contained in tetrapyrrole groups of the electron transport chains by photons in the sulfate reduction pathway reversed this pathway, yielding excess energy and an evolutionary incentive toward photosynthesis. Others have surmised that the first forms of photosynthesis used the *Sqr* genes to oxidize sulfides to elemental sulfur (Martin et al. 2018) but the shared presence of the *Sat*, *Apr* and *Dsr* genes in the metabolism ancestral to sulfur oxidation suggests that sulfur oxidation begin with sulfate as the end product (Hipp et al. 1997).

Whereas microbial sulfur reduction within the confines of volcanic vents may have been electron donor limited (depending on vent temperature and oxygen fugacity), with the advent of the first photosynthetic organisms this situation on the periphery would have been reversed. Sulfur reducers in the periphery of the vent system could use biogenic sulfate as an electron acceptor to remineralize organic matter (Bontognali et al. 2012), but further away from the vent, sulfate would be dropped out of the water column as insoluble barium sulfate (barite). Sulfur reducers can use sulfates bound in barites, but this happens slowly resulting in MSR becoming electron acceptor limited. This selective pressure was placed on sulfur reducers to use an alternative form of sulfur (elemental sulfur) to carry out remineralization; MIF sulfur isotopes show that this was provided by atmospheric aerosols but only began to manifest itself after Eoarchean time.

Low-temperature volcanic vents produce far more reduced sulfur than oxidized species (Nakamura and Takai 2014) which means that sulfur oxidation outpaces reduction . We hypothesize that this would result in most of the organic carbon produced by photosynthesis being emitted into the surrounding waters as opposed to being remineralized in the periphery of the vent. This accounts for the observed preference for elemental sulfur over sulfate by sulfur reducers in the multiple sulfur isotope data for the Archean.

In the ferruginous Archean oceans, lacking the ability to oxidize sulfides bound in pyrite would have contracted the threshold between limitation and complete inhibition in sulfur oxidizers, resulting in less electron donor limited primary production. This, along with the lack of precursor enzyme that could be readily adapted to metabolize elemental sulfur means that sulfur oxidizers required a greater quantity of changes while having less selective pressure than sulfur reducers to utilize elemental sulfur.

Our narrative is merely one explanation for the multiple sulfur isotope patterns observed in Eo- to Paleoarchean rocks; there are many unknowns. Future work might consider:

- What are the $^{13}C/^{12}C$ values of organic carbon from a hydrogenotrophic organism that uses the W–L pathway and an element other than a carbon compound as the electron acceptor (Schauder et al. 1988)?
- What changes would have to take place in the thiosulfate reductase enzyme to utilize elemental sulfur? The high sequence similarity between Psr and Phs suggests that few changes would be required (Duval et al. 2008) to occur but a detailed analysis of the active sites would be required to indicate how many amino acid substitutions had to take place (Galić et al. 2017).
- Do sulfur reducers use any biochemical tools to metabolize barium sulfate (barite)? Many microbes use chelating factors to metabolize solid-state materials (Thamdrup, 2000) for electron donors and acceptors. If sulfur reducers can obtain mineral-bound sulfate from barite it would raise the possibility that such an adaptation had yet to evolve in the Paleoarchean.
- Did the biochemistry of iron metabolism evolve from sulfur metabolism, or the other way around? As comparative molecular information has indicated that sulfur metabolism evolved from methanogenesis (Grein et al. 2013; Susanti and Mukhopadhyay 2012), such approaches may be used to understand the origins of iron metabolism.
- Attention ought to be directed at the timing of the appearance of photothiotrophy which we predict will be seen within the relatively under-represented geologic record from 3.75 to 3.5 Ga Eoarchean-Paleoarchean rocks. Specifically, a target for more detailed sampling should include sulfides of the Theespruit Formation in the Barberton Greenstone belt. It is between 3553 and 3547 Ma (Kröner et al. 1996) and composed mainly of volcanic ash with intermittent metamorphosed mudstone such as felsic schists.

Progress toward answering these questions would help enhance our understanding of how the early evolution of microbial metabolic systems, not just sulfur-based, can be reconciled with the Eoarchean to Paleoarchean geological record.

Acknowledgements

The ideas presented herein were clarified in the past several years by discussions with W. Adams, S. Benner, S. Flaxman, A. Kappler, K. Konhauser, M.J. Russell, D. Ritson, S. Smith, J. Sepúlveda, Y. Ueno, and B.A. Wing. We sincerely thank an anonymous reviewer for detailed comments and suggestions that improved this work. The opinions expressed in this publication are those of the authors, and do not necessarily reflect the views of the John Templeton Foundation. S.J.M. extends a special thanks to the Erwin Schrödinger International Institute for Mathematical Physics (Vienna, Austria) for a Visiting Scholar appointment during significant phases of the preparation of this manuscript.

Disclosure statement

The authors declare that they have no known competing financial interests or personal relationships that could have appeared to influence the work reported in this article. The authors declare the following financial interests/personal relationships which may be considered as potential competing interests. No potential conflict of interest was reported by the author(s).

Funding

P.R.M. was supported by the Department of Evolutionary Biology of the University of Colorado. Further support came from the Collaborative for Research in Origins (CRiO) directed by S.J.M. and supported by The John Templeton Foundation (principal investigator: S. Benner/FfAME/Award #54466).

ORCID

Stephen J. Mojzsis http://orcid.org/0000-0003-0000-125X

References

Alleon J, Summons RE. 2019. Organic geochemical approaches to understanding early life. Free Radic Biol Med 140:103–112.

Allwood AC, Rosing MT, Flannery DT, Hurowitz JA, Heirwegh CM. 2018. Reassessing evidence of life in 3,700-million-year-old rocks of Greenland. Nature 563(7730):241–244.

Arden TV. 1950. The solubility products of ferrous and ferrosic hydroxides. J Chem Soc. 179:882.doi:10.1039/jr9500000882.

Arndt NT, Nisbet EG. 2012. Processes on the young earth and the habitats of early life. Annu Rev Earth Planet Sci 40(1):521–549.

Arrhenius GO. 2003. Crystals and life. HCA. 86(5):1569–1586.

Avetisyan K, Buchshtav T, Kamyshny A. 2019. Kinetics and mechanism of polysulfides formation by a reaction between hydrogen sulfide and orthorhombic elemental sulfur. Geochim Cosmochim Acta 247: 96–105.

Bak F, Pfennig N. 1987. Chemolithotrophic growth of *Desufvibrio sulfodismutans* sp. nov. by disproportionation of inorganic sulfur compounds. Arch Microbiol 147(2):184–189.

Baroni M, Thiemens MH, Delmas RJ, Savarino J. 2007. Mass-independent sulfur isotopic compositions in stratospheric volcanic eruptions. Science 315(5808):84–87.

Bekker A, Barley ME, Fiorentini ML, Rouxel OJ, Rumble D, Beresford SW. 2009. Atmospheric sulfur in Archean komatiite-hosted nickel deposits. Science 326(5956):1086–1089.

Bell EA, Boehnke P, Harrison TM, Mao WL. 2015. Potentially biogenic carbon preserved in a 4.1 billion-year-old zircon. Proc Natl Acad Sci USA 112(47):14518–14521.

Benner SA, Bell EA, Biondi E, Brasser R, Carell T, Kim H-J, Mojzsis SJ, Omran A, Pasek MA, Trail D. 2020. When did life likely emerge on earth in an RNA-first process? Chem Syst Chem 2(2):e1900035.

Berner RA. 1970. Sedimentary pyrite formation. Am J Sci 268(1):1–23.

Berner RA. 1984. Sedimentary pyrite formation – an update. Geochim Cosmochim Acta 48(4):605–615.

Bontognali TRR, Sessions AL, Allwood AC, Fischer WW, Grotzinger JP, Summons RE, Eiler JM. 2012. Sulfur isotopes of organic matter preserved in 3.45-billion-year-old stromatolites reveal microbial metabolism. Proc Natl Acad Sci USA 109(38):15146–15151.

Braakman R, Smith E. 2012. The emergence and early evolution of biological carbon-fixation. PLoS Comput Biol 8(4):e1002455.

Canfield DE, Teske A. 1996. Late proterozoic rise in atmospheric oxygen concentration inferred from phylogenetic and sulphur-isotope studies. Nature 382(6587):127–132.

Canfield DE, Thamdrup B, Fleischer S. 1998. Isotope fractionation and sulfur metabolism by pure and enrichment cultures of elemental sulfur-disproportionating bacteria. Limnol Oceanogr 43(2):253–264.

Canfield DE, Thamdrup B. 1994. The production of ^{34}S-depleted sulfide during bacterial disproportionation of elemental sulfur. Science 266:1973–1975.

Canfield DE, Thamdrup B. 1996. Fate of elemental sulfur in an intertidal sediment. FEMS Microbiol Ecol 19(2):95–103.

Canfield DE. 2001. Biogeochemistry of sulfur isotopes. Rev Mineral Geochem 43(1):607–636.

Claire MA, Kasting JF, Domagal-Goldman SD, Stüeken EE, Buick R, Meadows VS. 2014. Modeling the signature of sulfur mass-independent fractionation produced in the Archean atmosphere. Geochim Cosmochim Acta 141:365–380.

Claypool GE, Mancini EA. 1989. Geochemical relationships of petroleum in Mesozoic reservoirs to carbonate source rocks of Jurassic Smackover Formation, southwestern Alabama. Am Assoc Petroleum Geol Bull 73:904–924.

Crowe SA, Paris G, Katsev S, Jones C, Kim S-T, Zerkle AL, Nomosatryo S, Fowle DA, Adkins JF, Sessions AL, et al. 2014. Sulfate was a trace constituent of Archean seawater. Science 346(6210):735–739.

Cypionka H, Smock AM, Bottcher ME. 1998. A combined pathway of sulfur compound disproportionation in *Desulfovivrio desulfuricans*. FEMS Microbio Lett 166(2):181–186.

Dahl C. 2017. Sulfur metabolism in phototrophic bacteria. In: Hallenbeck, PC, editor. Modern Topics in the Phototrophic Prokaryotes. Cham: Springer International, p27–66.

Dhillon A, Goswami S, Riley M, Teske A, Sogin M. 2005. Domain evolution and functional diversification of sulfite reductases. Astrobio 5(1):18–29.

Ding T, Valkiers S, Kipphardt H, De Bièvre P, Taylor PDP, Gonfiantini R, Krouse R. 2001. Calibrated sulfur isotope abundance ratios of three IAEA sulfur isotope reference materials and V-CDT with reassessment of the atomic weight of sulfyur. Geochim Cosmochim Acta 65(15):2433–2437.

Dodd MS, Papineau D, Grenne T, Slack JF, Rittner M, Pirajno F, O'Neil J, Little CTS. 2017. Evidence for early life in Earth's oldest hydrothermal vent precipitates. Nature 543(7643):60–64.

Domagal-Goldman S, Poirier B, Wing B. 2011. Mass-independent fractionation of sulfur isotopes: carriers and sources. NASA Workshop Report , Alexandria, VA, p. 36.

Dudley MW, Frost JW. 1994. Biocatalytic desulfurization of arylsulfonates. Bioorg Med Chem 2(7):681–690.

Duval S, Ducluzeau A-L, Nitschke W, Schoepp-Cothenet B. 2008. Enzyme phylogenies as markers for the oxidation state of the environment: the case of respiratory arsenate reductase and related enzymes. BMC Evol Biol 8:206.

Eickmann B, Hofmann A, Wille M, Bui TH, Wing BA, Schoenberg R. 2018. Isotopic evidence for oxygenated Mesoarchean shallow oceans. Nature Geosci 11(2):133–138.

Falkowsi PG. 2006. Evolution. tracing oxygen's imprint on earth's metabolic evolution. Science 311:1724–1725.

Falkowski PG, Raven JA. 2007. Aquatic photosynthesis, 2nd edition. Princeton: Princeton University Press.

Farquhar J, Bao H, Thiemens M. 2000. Atmospheric influence of earth's earliest sulfur cycle. Science 289(5480):756–759.

Farquhar J, Johnston DT, Wing BA, Habicht KS, Canfield DE, Airieau S, Thiemens MH. 2003. Multiple sulphur isotopic interpretations of

biosynthetic pathways: implications for biological signatures in the sulphur isotope record. Geobiology 1(1):27–36.
Farquhar J, Savarino J, Airieau S, Thiemens MH. 2001. Observation of wavelength-sensitive mass-independent sulfur isotope effects during SO_2 photolysis: implications for the early atmosphere. J Geophys Res 106(E12):32829–32839.
Farquhar J, Wing BA. 2003. Multiple sulfur isotopes and the evolution of the atmosphere. Earth Planet Sci Lett 213(1–2):1–13.
Fike DA, Bradley AS, Rose CV. 2015. Rethinking the ancient sulfur cycle. Annu Rev Earth Planet Sci 43(1):593–622.
Fike DA, Grotzinger JP, Pratt LM, Summons RE. 2006. Oxidation of the Ediacaran Ocean. Nature 444(7120):744–747.
Fike DA, Grotzinger JP. 2008. A paired sulfate–pyrite $\delta^{34}S$ approach to understanding the evolution of the Ediacaran-Cambrian sulfur cycle. Geochim Cosmochim Acta 72(11):2636–2648.
Finster K, Liesack W, Thamdrup B. 1998. Elemental sulfur and thiosulfate disproportionation by *Desulfocapsa sulfoexigens* sp. nov., a new anaerobic bacterium isolated from marine surface sediment. Appl Environ Microbiol 64(1):119–125.
Franz B, Lichtenberg H, Hormes J, Modrow H, Dahl C, Prange A. 2007. Utilization of solid "elemental" sulfur by the phototrophic purple sulfur bacterium *Allochromatium vinosum*: a sulfur K-edge X-ray absorption spectroscopy study. Microbiology (Reading, Engl)) 153(Pt 4):1268–1274.
Galić A, Mason PRD, Mogollón JM, Wolthers M, Vroon PZ, Whitehouse MJ. 2017. Pyrite in a sulfate-poor Paleoarchean basin was derived predominantly from elemental sulfur: evidence from 3.2 Ga sediments in the Barberton Greenstone Belt, Kaapvaal Craton. Chem Geol 449:135–146.
Gartman A, Luther GW. III, 2013. Comparison of pyrite (FeS_2) synthesis mechanisms to reproduce natural FeS_2 nanoparticles found at hydrothermal vents. Geochim Cosmochim Acta 120:447–458.
Génin J-MR, Bourrié G, Trolard F, Abdelmoula M, Jaffrezic A, Refait P, Maitre V, Humbert B, Herbillon A. 1998. Thermodynamic equilibria in aqueous suspensions of synthetic and natural Fe(II)−Fe(III) green rusts: occurrences of the mineral in hydromorphic soils. Environ Sci Technol 32(8):1058–1068.
Ghosh W, Mallick S, DasGupta SK. 2009. Origin of the *Sox* multienzyme complex system in ancient thermophilic bacteria and coevolution of its constituent proteins. Res Microbiol 160(6):409–420.
Gill BC, Lyons TW, Young SA, Kump LR, Knoll AH, Saltzman MR. 2011. Geochemical evidence for widespread euxinia in the later Cambrian ocean. Nature 469(7328):80–83.
Goldford JE, Hartman H, Marsland R, III, Segrè D. 2019. Environmental boundary conditions for the origin of life converge to an organo-sulfur metabolism. Nat Ecol Evol 3(12):1715–1724.
Goldhaber MB, Kaplan IR. 1975. Controls and consequences of sulfate reduction rates in recent marine sediments. Soil Sci 119:42–55.
Greer J, Caro G, Cates NL, Tropper P, Bleeker W, Kelly NM, Mojzsis SJ. 2020. Polyphase Archean granitoid gneisses and supracrustal enclaves of the southern Inukjuak Domain, Quebec (Canada). Lithos 364–365:105520.
Gregersen LH, Bryant DA, Frigaard N-U. 2011. Mechanisms and evolution of oxidative sulfur metabolism in green sulfur bacteria. Front Microbiol 2:116.
Grein F, Ramos AR, Venceslau SS, Pereira IAC. 2013. Unifying concepts in anaerobic respiration: insights from dissimilatory sulfur metabolism. Biochim Biophys Acta 1827(2):145–160.
Guy BM, Ono S, Gutzmer J, Kaufman AJ, Lin Y, Fogel ML, Beukes NJ. 2012. A multiple sulfur and inorganic carbon isotope record from non-conglomeratic sedimentary rocks of the Mesoarchean Witwatersrand Supergroup. South Afr Precamb Res 216-219: 208–231.
Habicht KS, Canfield DE, Rethmeier J. 1998. Sulfur isotope fractionation during bacterial reduction and disproportionation of thiosulfate and sulfite. Geochim Cosmochim Acta 62(15):2585–2595.
Habicht KS, Gade M, Thamdrup B, Berg P, Canfield D. E. 2002. Calibration of sulfate levels in the Archean ocean. Science 298(5602):2372–2374.
Halevy I, Alesker M, Schuster EM, Popovitz-Biro R, Feldman Y. 2017. A key role for green rust in the Precambrian oceans and the genesis of iron formations. Nature Geosci 10(2):135–139.
Harrison AG, Thode HG. 1958. Mechanisms of bacterial reduction of sulfate from isotope fractionation studies. Trans Faraday Soc 54: 84–92.
Hattori K, Cabri LJ. 1992. Origin of platinum-group mineral nuggets inferred from an Osmium-isotope study. Can Mineral 30:289–301.
Hattori K, Cameron EM. 1986. Archaean magmatic sulphate. Nature 319(6048):45–47.
Hattori S, Schmidt JA, Johnson MS, Danielache SO, Yamada A, Ueno Y, Yoshida N. 2013. SO2 photoexcitation mechanism links mass-independent sulfur isotopic fractionation in cryospheric sulfate to climate impacting volcanism. Proc Natl Acad Sci USA 110(44): 17656–17661.
Havig JR, Hamilton TL, Bachan A, Kump LR. 2017. Sulfur and carbon isotopic evidence for metabolic pathway evolution and a four-stepped Earth system progression across the Archean and Paleoproterozoic. Earth Sci Rev 174:1–21.
Heinzinger NK, Fujimoto SY, Clark MA, Moreno MS, Barrett EL. 1995. Sequence analysis of the phs operon in *Salmonella typhimurium* and the contribution of thiosulfate reduction to anaerobic energy metabolism. J Bacteriol 177(10):2813–2820.
Hipp WM, Pott AS, Thum-Schmitz N, Faath I, Dahl C, Trüper HG. 1997. Towards the phylogeny of APS reductases and sirohaem sulfite reductases in sulfate-reducing and sulfur-oxidizing prokaryotes. Microbiol 143(9):2891–2902.
Holland HD. 1973. The oceans: a possible source of iron in iron-formations. Econ Geol 68(7):1169–1172.
Holland HD. 1984. The chemical evolution of the atmospheres and oceans. Princeton Series in Geochemistry, Princeton: Princeton University Press.
Holland HD. 2006. The oxygenation of the atmosphere and oceans. Philos Trans R Soc Lond B Biol Sci 361(1470):903–915.
Holliday GL, Thornton JM, Marquet A, Smith AG, Rébeillé F, Mendel R, Schubert HL, Lawrence AD, Warre MJ. 2007. Evolution of enzymes and pathways for the biosynthesis of cofactors. Nat Prod Rep 24(5):972–987.
Hoshyaripour G, Hort M, Langmann B. 2012. How does the hot core of a volcanic plume control the sulfur speciation in volcanic emission? Geochem Geophys Geosys 13:Q07004.
Hulston JR, Thode HG. 1965. Variations in the S^{33}, S^{34} and S^{36} contents of meteorites and their relation to chemical and nuclear effects. J Geophys Res 70(14):3475–3484.
Izon G, Zerkle AL, Zhelezinskaia I, Farquhar J, Newton RJ, Poulton SW, Eigenbrode JL, Claire MW. 2015. Multiple oscillations in Neoarchean atmospheric chemistry. Earth Planet Sci Lett 431: 264–273.
Jacobsen SB, Pimentel-Klose MR. 1988. Nd isotopic variations in Precambrian banded iron formations. Geophys Res Lett 15(4): 393–396.
James HL. 1954. Sedimentary facies of iron-formation. Econ Geol 49: 236–294.
Jamieson JW, Wing BA, Farquhar J, Hannington MD. 2013. Neoarchean seawater sulphate concentrations from sulphur isotopes in massive sulphide ore. Nat Geosci 6(1):61–64.
Jamieson JW, Wing BA, Hannington MD, Farquhar J. 2006. Evaluating isotopic equilibrium among sulphide mineral pairs in Archean ore deposits: case study from the Kidd Creek VMS deposit, Ontario, Canada. Econ Geol 101(5):1055–1061.
Janecky DR, Shanks WC. 1988. Computational modelling of chemical and sulfur isotope reactions processes in seafloor hydrothermal systems: chimneys, massive sulfides and subjacent alteration zones. Can Mineral 26:805–825.
Johnston DT, Farquhar J, Wing BA, Kaufman A, Canfield DE, Habicht KS. 2005. Multiple sulfur isotope fractionations in biological systems: a case study with sulfate reducers and sulfur disproportionators. Am J Sci 305(6–8):645–660.
Johnston DT. 2011. Multiple sulfur isotopes and the evolution of Earth's surface sulfur cycle. Earth Sci Rev 106(1–2):161–183.

Jones GE, Starkey RJ. 1957. Fractionation of isotopes of sulfur my micro-organisms and their role in the deposition of native sulfur. J Appl Env Microbiol 5(2):111–115.
Jørgensen BB, Zawacki LX, Jannasch HW. 1990. Thermophilic bacterial sulfate reduction in deep-sea sediments at the Guaymas Basin hydrothermal vent site. Deep Sea Res 37(4):695–710.
Kafantaris F-CA, Druschel GK. 2020. Kinetics of the nucleophilic dissolution of hydrophobic and hydrophilic elemental sulfur sols by sulfide. Geochim Cosmochim Acta 269:554–565.
Kamber BS, Whitehouse MJ. 2006. Micro-scale sulphur isotope evidence for sulphur cycling in the late Archean shallow ocean. Geobiology 0(0):061221060249002–061221060249017.
Kamyshny A, Goifman A, Rizkov D, Lev O. 2003. Kinetics of disproportionation of inorganic polysulfides in undersaturated aqueous solutions at environmentally relevant conditions. Aquat Geochem 9(4):291–304.
Kaplan IR, Rittenberg SC. 1964. Microbiological fractionation of sulphur isotopes. J gen Micro 34:195–212.
Kappler A, Pasquero C, Konhauser KO, Newman DK. 2005. Deposition of banded iron formations by anoxygenic phototrophic Fe(II)-oxidizing bacteria. Geol 33(11):865–868.
Kaufman AJ, Johnston DT, Farquhar J, Masterson AL, Lyons TW, Bates S, Anbar AD, Arnold GL, Garvin J, Buick R. 2007. Late Archean biospheric oxygenation and atmospheric evolution. Science 317(5846):1900–1903.
Kelley DS, Karson JA, Blackman DK, Früh-Green GL, Butterfield DA, Lilley MD, Olson EJ, Schrenk MO, Roe KK, Lebon GT, et al. 2001. An off-axis hydrothermal vent field near the Mid-Atlantic Ridge at 30° N. Nature 412(6843):145–149. doi:10.1038/35084000.
King GM. 1984. Utilization of hydrogen, acetate, and "noncompetitive"; substrates by methanogenic bacteria in marine sediments. Geomicrobiol J 3(4):275–306.
Kiyosu Y. 1980. Chemical reduction and sulfur isotope effects of sulfate by organic matter under hydrothermal conditions. Chem Geol 30(1–2):47–56.
Klein C. 2005. Some precambrian banded iron formations (BIFs) from around the world: their age, geologic setting, mineralogy, metamorphism, geochemistry, and origin. Am Mineral 90(10):1473–1499.
Konhauser KO, Lalonde S, Amskold L, Holland HD. 2007. Was there really an Archean phosphate crisis? Science 315(5816):1234.
Krapež B, Barley ME, Pickard AL. 2003. Hydrothermal and resedimented origins of the precursor sediments to banded iron formation: sedimentological evidence from the Early Paleoproterozoic Brockman Supersequence of Western Australia. Sedimentology 50(5):979–1011.
Kröner A, Hegner E, Wendt JI, Byerly GR. 1996. The oldest part of the Barberton granitoid-greenstone terrain, South Africa: evidence for crust formation between 3.5 and 3.7 Ga. Precamb Res 78(1–3): 105–124.
Kuma K, Paplawsky W, Gedulin B, Arrhenius G. 1989. Mixed-valence hydroxides as bioorganic host minerals. Origins Life Evol Biosphere 19(6):573–602.
Kumar M, Francisco JS. 2016. Elemental sulfur aerosol-forming mechanism. Proc Natl Acad Sci USA 114(5):864–869.
Lasaga AC, Otake T, Watanabe Y, Ohmoto H. 2008. Anomalous fractionation of sulfur isotopes during heterogeneous reactions. Earth Planet Sci Lett 268(1–2):225–238.
Laska S, Lottspeich F, Kletzin A. 2003. Membrane-bound hydrogenase and sulfur reductase of the hyperthermophilic and acidophilic archaeon *Acidianus ambivalens*. Microbiology (Reading, Engl) 149(Pt 9):2357–2371.
Lebrun E, Brugna M, Baymann F, Muller D, Lièvremont D, Lett M-C, Nitschke W. 2003. Arsenite oxidase, an ancient bioenergetic enzyme. Mol Bio Evol 20(5):686–693.
Luther GQ, III, Findlay AJ, MacDonald DJ, Owings SM, Hanson TE, Beinart RA, Girguis PR. 2011. Thermodynamics and kinetics of sulfide oxidation by oxygen: a look at inorganically controlled reactions and biologically mediated processes in the environment. Front Microbiol 2:62.
Luther GQ. III, 1990. The frontier molecular-orbital theory approach in geochemical processes. In: Stumm, W, editor. Aquatic Chemical Kinetics. New York: John Wiley & Sons, p173–198.
Lyons JR. 2009. Atmospherically-derived mass-independent sulfur isotope signature, and incorporation into sediments. Chem Geol 267(3–4):164–174.
Lyons TW, Reinhard CT, Planavsky NJ. 2014. The rise of oxygen in Earth's early ocean and atmosphere. Nature 506(7488):307–315.
Machel HG. 1998. Gas souring by thermochemical sulfate reduction at 140 °C: discussion. Am Assoc Petroleum Geol Bull 82:1870–1873.
Maier RM. 2014. Biogeochemical cycling. chapter 16. In environmental microbiology, 3rd edition. San Diego, CA: Academic Press, pp.339–373.
Martin WF, Bryant DA, Beatty JT. 2018. A physiological perspective on the origin and evolution of photosynthesis. FEMS Microbiol Rev 42(2):205–231.
Martin WF, Russell MJ. 2007. On the origin of biochemistry at an alkaline hydrothermal vent. Philos Trans R Soc Lond B Biol Sci 362(1486):1887–1925.
Martin WF, Sousa FL. 2015. Early microbial evolution: the age of anaerobes. Cold Spring Harb Perspect Biol 8(2):a018127.
Martin WF. 2016. Physiology, phylogeny and the energetic roots of life. Period Biol 118(4):343–352.
Melton ED, Sorokin DY, Overmars L, Chertkov O, Clum A, Pillay M, Ivanova N, Shapiro N, Kyrpides NC, Woyke W, et al. 2016. Complete genome sequence of *Desulfurivibrio alkaliphilus* strain AHT2 T, a haloalkaliphilic sulfidogen from Egyptian hypersaline alkaline lakes. Stand Genom Sci 11:67.
Meyer B, Kuever J. 2007. Molecular analysis of the distribution and phylogeny of dissimilatory adenosine-5'-phosphosulfate reductase-encoding genes (aprBA) among sulfur-oxidizing prokaryotes. Microbiology (Reading, Engl) 153(Pt 10):3478–3498.
Mojzsis SJ, Arrhenius G, McKeegan KD, Harrison TM, Nutman AP, Friend CRL. 1996. Evidence for life on earth before 3,800 million years ago. Nature 384(6604):55–59.
Mojzsis SJ, Coath CD, Greenwood JP, McKeegan KD, Harrison TM. 2003. Mass independent isotope effects in Archean (2.5 to 3.8 Ga) sedimentary sulfides determined by ion microprobe analysis. Geochim Cosmochim Acta 67(9):1635–1658.
Mojzsis SJ. 2007. Sulphur on the early earth. Dev Precamb Geol 15: 923–970.
Monster J, Appel PWU, Thode HG, Schidlowski M, Carmichael CM, Bridgwater D. 1979. Sulfur isotop studies in early Archean sediments from Isua, West Greenland: implications for the antiquity of bacterial sulfate reduction. Geochim Cosmochim Acta 43(3): 405–413.
Morita RY. 1999. Is H_2 the universal energy source for long-term survival? Microb Ecol 38(4):307–320.
Müller AL, Kjeldsen KU, Rattei T, Pester M, Loy A. 2015. Phylogenetic and environmental diversity of DsrAB-type dissimilatory (bi)sulfite reductases. Isme J 9(5):1152–1165.
Nakamura K, Takai K. 2014. Theoretical constraints of physical and chemical properties of hydrothermal fluids on variations in chemolithotrophic microbial communities in seafloor hydrothermal systems. Prog Earth Planet Sci 1(1):5.
Newton RC, Manning CM. 2004. Solubility of anhydrite, $CaSO_4$, in NaCl-H_2O solutions at high pressures and temperatures: applications to fluid-rock interaction. J Petrol 46(4):701–716.
Nutman AP, Bennett VC, Friend CRL, Van Kranendonk MJ, Chivas AR. 2016. Rapid emergence of life shown by discovery of 3,700-million-year-old microbial structures. Nature 537(7621):535–538.
Nutman AP, Mojzsis SJ, Friend CRL. 1997. Identification of the oldest water-lain sediments at >3850 Ma from Akilia island, southern West Greenland: Geochim Cosmochim Acta 61:2475–2484.
Olson JM. 2006. Photosynthesis in the Archean era. Photosyn Res 88(2):109–117.
Ono S, Eigenbrode JL, Pavlov AA, Kharecha P, Rumble D, Kasting JF, Freeman KH. 2003. New insights into Archean sulfur cycle from mass-independent sulfur isotope records from the Hamersley Basin, Australia. Earth Planet Sci Lett 213(1–2):15–30.

Ono S, Whitehill AR, Lyons JR. 2013. Contribution of isotopologue self-shielding to sulfur mass independent fractionation during sulfur dioxide photolysis. J Geophys Res Atmos 118(5):2444–2454.
Ono S, Wing B, Johnston D, Farquhar J, Rumble D. 2006. Mass-dependent fractionation of quadruple stable sulfur isotope system as a new tracer of sulfur biogeochemical cycles. Geochim Cosmochim Acta 70(9):2238–2252.
Orsi WD, Schink B, Buckel W, Martin WF. 2020. Physiological limits to life in anoxic subseafloor sediment. FEMS Microbiol Rev 44(2): 219–231.
Pace N. 2006. Time for a change. Nature 441(7091):289.
Papineau D, De Gregorio BT, Cody GD, Fries MD, Mojzsis SJ, Steele A, Rhonda M, Stroud RM, Fogel ML. 2010. Ancient graphite in the Eoarchean quartz-pyroxene rocks from Akilia in southern West Greenland II: isotopic and chemical compositions and comparison with Paleoproterozoic banded iron formations. Geochim Cosmochim Acta 74(20):5884–5905.
Papineau D, Mojzsis SJ, Coath CD, Karhu JA, McKeegan KD. 2005. Multiple sulfur isotopes of sulfides from sediments in the aftermath of Paleoproterozoic glaciations. Geochim Cosmochim Acta 69(21): 5033–5060.
Papineau D, Mojzsis SJ, Schmitt AK. 2007. Multiple sulfur isotopes from Paleoproterozoic Huronian interglacial sediments and the rise of atmospheric oxygen. Earth Planet Sci Lett 255(1–2):188–212.
Paris G, Adkins JF, Sessions AL, Webb SM, Fischer WW. 2014. Neoarchean carbonate-associated sulfate records positive 33S anomalies. Science. 346(6210):739–741. doi:10.1126/science.1258211.
Pavlov AA, Kasting JF. 2002. Mass-independent fractionation of sulfur isotopes in Archean sediments: strong evidence for an anoxic Archean atmosphere. Astrobiology 2(1):27–41.
Philippot P, Va Zuilen M, Lepot K, Thomazo C, Farquhar J, Van Kranendonk MJ. 2007. Early Archaean microorganisms preferred elemental sulfur, not sulfate. Science 317(5844):1534–1537.
Posth NR, Konhauser KO, Kappler A. 2013. Microbial processes in banded iron formation deposition. Sedimentology 60(7):1733–1754.
Preiner M, Igarashi K, Muchowska KB, Yu M, Varma SJ, Kleinermanns K, Nobu MK, Kamagata Y, Tüysüz H, Moran J, et al. 2020. A hydrogen-dependent geochemical analogue of primordial carbon and energy metabolism. Nat Ecol Evol 4(4):534–542.
Proskurowski G, Lilley MD, Seewald JS, Früh-Green GL, Olson EJ, Lupton JE, Sylva SP, Kelley DS. 2008. Abiogenic hydrocarbon production at Lost City hydrothermal field. Science 319(5863):604–607.
Pyzik AJ, Sommer SE 1981. Sedimentary iron monosulfide: Kinetics and mechanism of formation. Geochim Cosmochim Acta 45(5): 687–698.
Rabus R, Hansen TA, Widdel F. 2013. Dissimilatory sulfate-and sulfur-reducing prokaryotes. In: Rosenberg E, DeLong EF, Stackebrandt, E, Lory S, Thompson, F, editors. The Prokaryotes: Prokaryotic Physiology and Biochemistry, Heidelberg: Springer, p309–404.
Ranjan S, Todd ZR, Sutherland JD, Sasselov DD. 2018. Sulfidic anion concentrations on early earth for surficial origins-of-life chemistry. Astrobio 18(8):1023–1040.
Riciputi LR, Paterson BA, Ripperdan RL. 1998. Measurement of light stable isotope ratios by SIMS: matrix effects for oxygen, carbon and sulfur isotopes in minerals. Int J Mass Spectrom 178:81–112.
Rawlings DE, Tributsch H, Hansford GS. 1999. Reasons why 'Leptospirillum'-like species rather than *Thiobacillus ferrooxidans* are the dominant iron-oxidizing bacteria in many commercial processes for the biooxidation of pyrite and related ores. Microbiology 145(1):5–13.
Rickard D, Luther GW. 2007. Chemistry of iron sulfides. Chem Rev 107(2):514–562.
Rimmer PB, Shorttle O. 2019. Origin of life's building blocks in carbon- and nitrogen-rich surface hydrothermal vents. Life 9(1):12.
Romero AB, Thiemens MH. 2003. Mass-independent sulfur isotopic compositions in present-day sulfate aerosols. J Geophy Res Atmos 108:4524.
Rosing MT. 1999. ^{13}C-Depleted carbon microparticles in >3700-Ma sea-floor sedimentary rocks from West Greenland. Science 283(5402):674–676.
Russell MJ, Martin W. 2004. The rocky roots of the acetyl coenzyme-A pathway. Trends Biochem Sci 29(7):358–363.
Russell MJ, Nitschke W, Branscomb E. 2013. The inevitable journey to being. Phil Trans R Soc B 368: 20120254. doi:10.1098/rstb
Sageman J, Jørgensen BB, Greef O. 1998. Temperature dependence and rates of sulfate reduction in cold sediments of Svalbard, Arctic Ocean. Geomicrobiol J 15(2):85–100.
Savarino J, Romero A, Cole-Dai J, Bekki S, Thiemens MH. 2003. UV induced mass-independent fractionations in stratospheric volcanic sulfate. Geophy Res Lett 30:1–4.
Scaillet B, Clemente B, Evans BW, Pichavant M. 1998. Redox control of sulfur degassing in silicic magmas. J Geophys Res 103(B10): 23937–23950.
Schauder R, Preu A, Jetten M, Fuchs G. 1988. Oxidative and reductive acetyl CoA/carbon monoxide dehydrogenase pathway in *Desulfobacterium autotrophicum. 2. De*monstration of the enzymes and comparison of CO dehydrogenase. Arch Microbiol 151(1):84–89.
Schidlowski M, Eichmann R, Junge CE. 1975. Precambrian sedimentary carbonates: carbon and oxygen isotope geochemistry and implications for the terrestrial oxygen budget. Precambrian Res 2(1):1–69.
Schidlowski M, Hayes JM, Kaplan IR. 1983. Isotopic inferences of ancient biochemistries: carbon, sulfur, hydrogen and nitrogen. In: Schopf JW, editor. Earth's earliest biosphere: its origin and evolution. New Jersey: Princeton University Press, p149–186.
Schidlowski M. 1982. Content and isotopic composition of reduced carbon in sediments. In: Holland HD, Schidlowski M, editors. Mineral deposition and the evolution of the biosphere. Dahlem Konferenzen. Berlin: Springer, p. 103–122.
Schidlowski M. 1988. A 3,800-million-year isotopic record of life from carbon in sedimentary rocks. Nature 333(6171):313–318.
Schink B. 1997. Energetics of syntrophic cooperation in methanogenic degradation. Microbiol Mol Bio Rev 61(2):262–280.
Schönheit P, Buckel W, Martin WF. 2016. On the origin of heterotrophy. Trends Microbiol 24(1):12–25.
Schoonen MAA, Barnes HL. 1991. Reactions forming pyrite and marcasite from solution: I. Nucleation of FeS2 below 100 °C. Geochim Cosmochim Acta 55(6):1495–1504.
Schut GJ, Boyd ES, Peters JW, Adams MW. 2013. The modular respiratory complexes involved in hydrogen and sulfur metabolism by heterotrophic hyperthermophilic archaea and their evolutionary implications. FEMS Microbiol Rev 37(2):182–203.
Segel IH, Renosto F, Seubert PA. 1987. Sulfate-Activating Enzymes. Meth Enzym 143:334–349.
Shen YA, Buick R, Canfield DE. 2001. Isotopic evidence for microbial sulphate reduction in the early Archaean era. Nature 410(6824):77–81.
Shen YN, Farquhar J, Masterson A, Kaufman AJ, Buick R. 2009. Evaluating the role of microbial sulfate reduction in the early Archean using quadruple isotope systematics. Earth Planet Sci Lett 279(3–4):383–391.
Sim MS, Ogata H, Lubitz W, Adkins JF, Sessions AL, Orphan VJ, McGlynn S. 2019. Role of APS reductase in biogeochemical sulfur isotope fractionation. Nature Commun 10:1–9.
Simon J, Kroneck PMH. 2013. Microbial sulfite respiration. Adv Microb Phys 62:45–117.
Sleep NH, Bird D. K. 2007. Niches of the pre-photosynthetic biosphere and geologic preservation of Earth's earliest ecology. Geobiology 5(2):101–117.
Sojo V, Herschy B, Whicher A, Camprubí E, Lane N. 2016. The origin of life in alkaline hydrothermal vents. Astrobiology 16(2):181–197.
Sousa FL, Preiner M, Martin WF. 2018. Native metals, electron bifurcation, and CO_2 reduction in early biochemical evolution. Curr Opin Microbiol 43:77–83.
Steudel R. 2003. Inorganic Polysulfides S_n^{2-} and Radical Anions $S_n^{\bullet-}$. In: Steudel R, editors. Topics in Current Chemistry. Elemental Sulfur and Sulfur-Rich Compounds II. Berlin: Springer.
Strauss H. 1993. The sulfur isotopic record of Precambrian sulfates – new data and a critical evaluation of the existing record. Precamb Res 63(3–4):225–246.
Strauss H. 1997. The isotopic composition of sedimentary sulfur through time. Palaeogeog Palaeoclimat Palaeoecol 132(1–4):97–118.
Strauss H. 2003. Sulphur isotopes and the early Archaean sulphur cycle. Precamb Res 126(3–4):349–361.

Susanti D, Mukhopadhyay B. 2012. An intertwined evolutionary history of methanogenic archaea and sulfate reduction. PLOS One 7(9): e45313.

Takai K, Gamo T, Tsunogai U, Nakayama N, Hirayama H, Nealson KH, Horikoshi K. 2004. Geochemical and microbiological evidence for a hydrogen-based, hyperthermophilic subsurface lithoautotrophic microbial ecosystem (HyperSLiME) beneath an active deep-sea hydrothermal field. Extremophiles 8(4):269–282.

Tashiro T, Ishida A, Hori M, Igisu M, Koike M, Méjean P, Takahata N, Sano Y, Komiya T. 2017. Early trace of life from 3.95 Ga sedimentary rocks in Labrador, Canada. Nature 549(7673):516–518.

Thamdrup B. 2000. Bacterial manganese and iron reduction in aquatic sediments. In: Schink B, editors, Advances in Microbial Ecology. 16th edn. New York, NY: Springer, pp 41.

Thamdrup B, Finster K, Fossing H, Hansen JW, Jørgensen BB. 1994. Thiosulfate and sulfite distribution in porewater marine sediments related to manganese, iron and sulfur geochemistry. Geochim Cosmochim Acta 58(1):67–73.

Thamdrup B, Finster K, Hansen JW, Bak F. 1993. Bacterial disproportionation of elemental sulfur coupled to chemical-reduction of iron or manganese. Appl Environ Microbiol 59(1):101–108.

Thauer RK, Kaster A-K, Seedorf H, Buckel W, Hedderich R. 2008. Methanogenic archaea: ecologically relevant differences in energy conservation. Nat Rev Microbiol 6(8):579–591.

Thiemens MH, Lin M. 2019. Use of isotope effects to understand the present and past of the atmosphere and climate and track the origin of life. Angew Chem Int Ed Engl 58(21):6826–6844.

Thode HG, Kleerekoper H, McElcheran D. 1951. Isotope fractionation in bacterial fractionation of sulphate. Research 4:581–582.

Thode HG, Macnamara J, Collins CB. 1949. Natural variations in the isotopic content of sulphur and their significance. Can J Res 27b(4): 361–373.

Thomassot E, O'Neil J, Francis D, Cartigny P, Wing BA. 2015. Atmospheric record in the Hadean Eon from multiple sulfur isotope measurements in Nuvvuagittuq Greenstone Belt (Nunavik, Quebec. Proc Natl Acad Sci USA 112(3):707–712.

Thomazo C, Pinti DL, Busigny V, Ader M, Hashizume K, Philippot P. 2009. Biological activity and the earth's surface evolution: Insights from carbon, sulfur, nitrogen and iron stable isotopes in the rock record. C R Palevol 8(7):665–678.

Trolard F, Génin J-MR, Abdelmoula M, Bourrié G, Humbert B, Herbillon A. 1997. Identification of a green rust mineral in a reductomorphic soil by Mossbauer and Raman spectroscopies. Geochim Cosmochim Acta 61(5):1107–1111.

Trudinger PA, Chambers LA, Smith JW. 1985. Low temperature sulphate reduction: biological vs. abiological. Can J Earth Sci 22(12): 1910–1918.

Ueno Y, Yamada K, Yoshida N, Maruyama S, Isozaki Y. 2006. Evidence from fluid inclusions for microbial methanogenesis in the early Archaean era. Nature 440(7083):516–518.

Urey HC. 1947. Thermodynamic properties of isotopic substances. J Chem Soc 562–581.

Urich TT, Bandeiras TM, Leal SS, Rachel R, Albrecht T, Zimmermann P, Scholz C, Teixeira M, Gomes CM, Kletzin A. 2004. The sulphur oxygenase reductase from *Acidianus ambivalens* is a multimeric protein containing a low-potential mononuclear non-haem iron centre. Biochem J 381(Pt 1):137–146.

Varma SJ, Muchowska KB, Chatelain P, Moran J. 2018. Native iron reduces CO_2 to intermediates and end-products of the acetyl CoA pathway. Nat Ecol Evol 2(6):1019–1024.

Wacey D, McLoughlin N, Whitehouse MJ, Kilburn MR. 2010. Two existing sulfur metabolisms in a ca. 3400 Ma sandstone. Geology 38(12):1115–1118.

Ward LM, Rasmussen B, Fischer WW. 2019. Primary productivity was limited by electron donors prior to the advent of oxygenic photosynthesis. J Geophys Res Biogeosci 124(2):211–226.

Watanabe Y, Farquhar J, Ohmoto H. 2009. Anomalous fractionations of sulfur isotopes during thermochemical sulfate reduction. Science 324(5925):370–373.

Watanabe Y, Farquhar J, Ohmoto H. 2009. Anomalous fractionations of sulfur isotopes during thermochemical sulfate reduction. Science 324(5925):370–373.

Watson EB, Cherniak DJ, Frank EB. 2009. Retention of biosignatures and mass-independent fractionations in pyrite: self-diffusion of sulfur. Geochim Cosmochim Acta 73(16):4792–4802.

Weiss MC, Sousa FL, Mrnjavac N, Neukirchen S, Roettger M, Nelson-Sathi S, Martin WF. 2016. The physiology and habitat of the last universal common ancestor. Nature Microbiol 1:16116.

Weissgerber T, Sylvester M, Kröninger L, Dahl C. 2014. A comparative quantitative proteomic study identifies new proteins relevant for sulfur oxidation in the purple sulfur bacterium *Allochromatium vinosum*. Appl Env Micriobiol. 80:2279–2292.

Whitehill AR, Ono S. 2012. Excitation band dependence of sulfur isotope mass-independent fractionation during photochemistry of sulfur dioxide using broadband light sources. Geochim Cosmochim Acta 94:238–253.

Whitehouse MJ, Dunkley DJ, Kusiak MA, Wilde SA. 2019. On the true antiquity of Eoarchean chemofossils – assessing the claim for earth's oldest biogenic graphite in the Saglek Block of Labrador. Precamb Res 323:70–81.

Whitehouse MJ, Myers JM, Fedo CM. 2009. The Akilia Controversy: field, structural and geochronological evidence questions interpretations of >3.8 Ga life in SW Greenland. J Geol Soc Lond 166(2): 335–348.

Whiticar MJ, Faber E. 1986. Methane oxidation in sediment and water column environments – isotope evidence. Org Geochem 10(4–6): 759–768.

Widdel F, Pfennig N. 1981. Studies on dissimilatory sulfate-reducing bacteria that decompose fatty acids. Arch Microbiol 129(5):395–400.

Xiong J. 2006. Photosynthesis: what color was its origin? Genome Biol 7(12):245.

Xu Y, Schoonen MAA, Nordstrom DK, Cunningham KM, Ball JW. 1998. Sulfur geochemistry of hydrothermal waters in Yellowstone National Park- I. The origin of thiosulfate in hot spring waters. Geochim Cosmochim Acta 62(23–24):3729–3743.

Young ED, Galy A, Nagahara H. 2002. Kinetic and equilibrium mass-dependent isotope fractionation laws in nature and their geochemical and cosmochemical significance. Geochim Cosmochim Acta 66(6):1095–1104.

Zawaski M, Kelly NM, Orlandini OM, Allwood AC, Nichols CIO, Mojzsis SJ. 2020. Reappraisal of purported ca. 3.7 Ga stromatolites from the Isua Supracrustal Belt (West Greenland) from detailed chemical and structural analysis. Earth Planet Sci Lett. 545:116409.

Zhelezinskaia I, Kaufman AJ, Farquhar J, Cliff J. 2014. Large sulfur isotope fractionations associated with Neoarchean microbial sulfate reduction. Science 346(6210):742–744.

Zopfi J, Ferdelman TG, Fossing H. 2004. Distribution and fate of sulfur intermediates—sulfite, tetrathionate, thiosulfate, and elemental sulfur in marine sediments. In: Amend JP, Edwards KJ, Lyons TW, editors. Sulfur biogeochemistry—Past and Present. Boulder, CO: Geological Society of America Special Paper, p. 97–116.